

The effect of *in vitro* culture conditions on cell metabolism



Fiona Hartley

St. Anne's College

University of Oxford

Thesis submitted for the degree of M.Sc. by Research

Trinity 2018

Abstract

Because cells have adapted to respond to their extracellular environment, the *in vitro* conditions under which cells are cultured have the potential to impact on cell metabolism. This study aims to investigate the effect of various components of culture medium on the metabolism of Chinese Hamster Ovary (CHO) cells.

Firstly, the effect of glucose and glutamine, two important carbon sources, was investigated. The impact of these nutrients on cell growth, viability, oxygen consumption rate (OCR) and steady state ATP levels was assessed. Glucose was found to have a suppressive effect on OCR, while under glucose limiting conditions, glutamine was able to enhance OCR. Although commonly considered a waste product, lactate can also act as a source of carbon and can be consumed by CHO cells. The effect of lactate on the above parameters was also measured, but no robust changes were observed.

Serum is added to the majority of cell culture media and is necessary for cell growth. However, since this product is animal derived, batch to batch variability is high and its composition is not well documented. The broad profile of components in serum means it has the potential to exert many effects on cells, but the effect serum of on cell metabolism is poorly understood. For this reason, the metabolic state of CHO cells in reduced serum was investigated using the aforementioned assays. Metabolite profiling was also performed using metabolomics. Cells cultured in 10% foetal bovine serum (FBS) were found to have a higher OCR than those cultured in both 1% and 0.1% FBS. This was supported by metabolite profiling which showed a greater abundance of tricarboxylic acid (TCA) cycle intermediates in these cells. The metabolite data also indicated increased oxidative stress in cells cultured in 10% FBS. Glucose metabolism also appeared to be affected, with a higher

abundance of early glycolytic and glycogenesis intermediates in cells cultured in low (0.1%) serum.

This study shows that both the substrates available in culture media and the commonly used supplement, FBS, can influence metabolic pathways within mammalian cells, meaning their effects must be accounted for, particularly in studies of metabolism.

Contents

Abstract.....	2
Contents.....	4
Abbreviations.....	6
List of Tables.....	9
List of Figures.....	10
1. Introduction.....	13
1.1 Glycolytic and Oxidative Metabolism.....	13
1.2 Metabolic Adaptation to the Extracellular Environment.....	15
1.3 <i>In Vitro</i> Culture.....	18
1.3.1 Glucose.....	19
1.3.2 Glutamine.....	21
1.3.3 Lactate.....	22
1.3.4 Serum.....	23
1.3.5 Oxygen.....	27
1.4 Aims.....	28
2. Materials and Methods.....	29
2.1 Culture of CHO cells.....	29
2.2 Seeding of CHO cells.....	29
2.3 Assessment of Cell Number using Hoechst.....	30
2.4 Assessment of Cell Death and Cell Number using Propidium Iodide (PI)...	30
2.5 Assessment of Total Cellular ATP.....	31
2.6 Assessment of Oxygen Consumption Rate (OCR).....	31
2.7 Growth Curve.....	33
2.8 Fluorescent Imaging.....	33
2.9 Phase Contrast Imaging.....	34
2.10 Metabolomics Sample Collection.....	34
2.11 DNA Extraction and Quantification.....	35
2.12 Metabolomics Liquid Chromatography and Mass Spectrometry.....	35
2.13 Data Analysis.....	37
2.14 Metabolomics Data Analysis.....	37
3. Results.....	39
3.1 Determination of the Linear Range for Cell Number Assays.....	40

3.2 The Effect of Glucose on the Metabolic Profile of CHO cells	42
3.3 The Effect of Glutamine on Cell Metabolism under Various Glucose Concentrations	45
3.4 The Effect of Lactate on Cell Metabolism.....	47
3.5 Visualisation of CHO cells	50
3.6 The Effect of Serum on the Phenotype and Metabolic Profile of CHO cells	52
3.7 Extraction of DNA from Pellets Collected during Metabolite Extraction - Method Development	55
3.8 Metabolomic Analysis of CHO cells in a Reduced Serum Environment.....	58
4. Discussion	72
4.1 Glucose	72
4.2 Glutamine.....	73
4.3 Lactate	74
4.4 FBS	76
5. Concluding Remarks	87
Acknowledgements	88
References	89

Abbreviations

- 4EBP1 - eukaryotic translation initiation factor 4E binding protein 1
- ADP - adenosine diphosphate
- AMP - adenosine monophosphate
- AMPK - AMP-activated protein kinase
- ANOVA - analysis of variance
- ANT - adenine nuclear translocase
- ATP - adenosine triphosphate
- CAP - catabolite activator protein
- CHO - Chinese hamster ovary
- ChREBP - carbohydrate responsive element binding protein
- CoA - coenzyme A
- DHAP - dihydroxyacetone phosphate
- DMEM - Dulbecco's Modified Eagle's medium
- DNA - deoxyribonucleic acid
- EDTA - ethylenediaminetetraacetic acid
- eIF4E - eukaryotic translation initiation factor 4E
- ETC - electron transport chain
- F16BP - fructose 1,6-bisphosphate
- FAD - flavin adenine dinucleotide
- FBS - foetal bovine serum
- FCCP - carbonyl cyanide-p-trifluoromethoxyphenylhydrazone
- GSH - reduced glutathione
- GSSG - oxidised glutathione

- HEK293 - human embryonic kidney cells 293
- HSD - honest significant difference
- IMDM - Iscove's Modified Dulbecco's Media
- LC – liquid chromatography
- LDH - lactate dehydrogenase
- MEM - Minimum Essential Medium
- mRNA - messenger RNA
- MS - mass spectrometry
- mTORC1 - mammalian target of rapamycin complex 1
- NAD - nicotinamide adenine dinucleotide
- NADPH - nicotinamide adenine dinucleotide phosphate
- OCR - oxygen consumption rate
- OXPHOS - oxidative phosphorylation
- PCA - principle component analysis
- PDH - pyruvate dehydrogenase
- PEPCK - phosphoenolpyruvate carboxykinase
- PI - propidium iodide
- RNA - ribonucleic acid
- ROS - reactive oxygen species
- RPMI - Roswell Park Memorial Institute medium
- siRNA - small interfering RNA
- TCA - tricarboxylic acid
- TE - Tris-EDTA
- TMRM - tetramethylrhodamine methyl ester
- TR-F - time resolved fluorescence

- UDP-glucose - uridine diphosphate-glucose
- v/v - volume per volume

List of Tables

Table 1 - Results of DNA quantification and quality assessment.

Table 2 - P values for the changes in metabolite abundance between 10%, 1% and 0.1% FBS cultures.

List of Figures

Figure 1 - Overview of glycolysis and the TCA cycle.

Figure 2 - Example plot showing fluorescence lifetime value against time.

Figure 3 - Determination of linear range when using Hoechst as a marker for cell number.

Figure 4 - Determination of linear range when using PI as a marker for viable cell number.

Figure 5 - Growth curve of CHO cells cultured in different glucose concentrations over 96 hours.

Figure 6 - The effect of glucose on ATP, OCR and cell number.

Figure 7 - The effect of glutamine on OCR, ATP and cell number in high glucose medium.

Figure 8 - The effect of glutamine on OCR, ATP and cell number under glucose limiting conditions.

Figure 9 - Experiment 1 showing the effect of lactate and glutamine on ATP, OCR and cell number.

Figure 10 - Experiment 2 showing the effect of lactate and glutamine on ATP, OCR and cell number.

Figure 11 - Field of view showing CHO cells co-stained with MitoTracker Green and TMRM.

Figure 12 - CHO cells stained with MitoTracker Green.

Figure 13 - CHO cells grown in varying serum concentrations and visualised using phase contrast microscopy.

Figure 14 - The effect of varying serum concentrations on ATP, OCR, cell number and cell death.

Figure 15 - The relative abundance of identified polar/ionic metabolites in cells from cultures containing 0.1% or 1% FBS.

Figure 16 - The relative abundance of identified polar/ionic metabolites in cells from cultures containing 0.1% or 10% FBS.

Figure 17 - The relative abundance of identified polar/ionic metabolites in cells from cultures containing 1% or 10% FBS.

Figure 18 - The relative abundance of identified amine-based molecules in cells from cultures containing 0.1% or 1% FBS.

Figure 19 - The relative abundance of identified amine-based molecules in cells from cultures containing 0.1% or 10% FBS.

Figure 20 - The relative abundance of identified amine-based molecules in cells from cultures containing 1% or 10% FBS.

Figure 21 – PCA of the metabolite profiles of 10%, 1% and 0.1% FBS cultures.

Figure 22 - Glycolysis, the TCA cycle and related intermediates: fold changes in 10% vs 0.1% FBS cultures.

Figure 23 - The abundance of proteinogenic amino acids.

Figure 24 - The abundance of glutathione and ATP in 10%, 1% and 0.1% FBS cultures.

Figure 25 - Amino acid catabolism pathways surrounding glutathione: fold changes in 10% vs 0.1% FBS cultures.

1. Introduction

1.1 Glycolytic and Oxidative Metabolism

There are two key ATP producing pathways in a typical eukaryotic cell: glycolysis and oxidative phosphorylation (OXPHOS). Glycolysis takes place in the cytoplasm and involves the breakdown of glucose into two pyruvate molecules (see Figure 1). Glycolytic flux is tightly controlled by three enzymes: hexokinase, phosphofructokinase and pyruvate kinase [2]. Feedback inhibition is a common regulatory mechanism which prevents the unnecessary breakdown of glucose. For example, hexokinase is inhibited by its product, glucose 6-phosphate [2]. The first steps of glycolysis involve utilisation of ATP, but this is regenerated in the second half of glycolysis resulting in an overall net gain of two ATP per glucose molecule [3]. NAD^+ is used to oxidise various metabolites in the pathway, resulting in the production of reduced NAD^+ as NADH. If glycolysis is carried out solely under anaerobic conditions, this NAD^+ must be replenished through the conversion of pyruvate to lactate with simultaneous conversion of NADH to NAD^+ . This reaction is catalysed by the enzyme lactate dehydrogenase (LDH).

Under aerobic conditions, pyruvate enters the mitochondria driving OXPHOS (see Figure 1). In the mitochondrial matrix, pyruvate dehydrogenase (PDH) catalyses the link reaction, decarboxylating pyruvate to acetyl CoA. Acetyl CoA undergoes a condensation reaction with oxaloacetate to form citrate and thus enters the tricarboxylic acid (TCA) cycle. Flux through the TCA cycle produces the reducing equivalents NADH and FADH_2 . These feed electrons into the electron transport chain (ETC), which is located on the inner mitochondrial membrane. Electrons

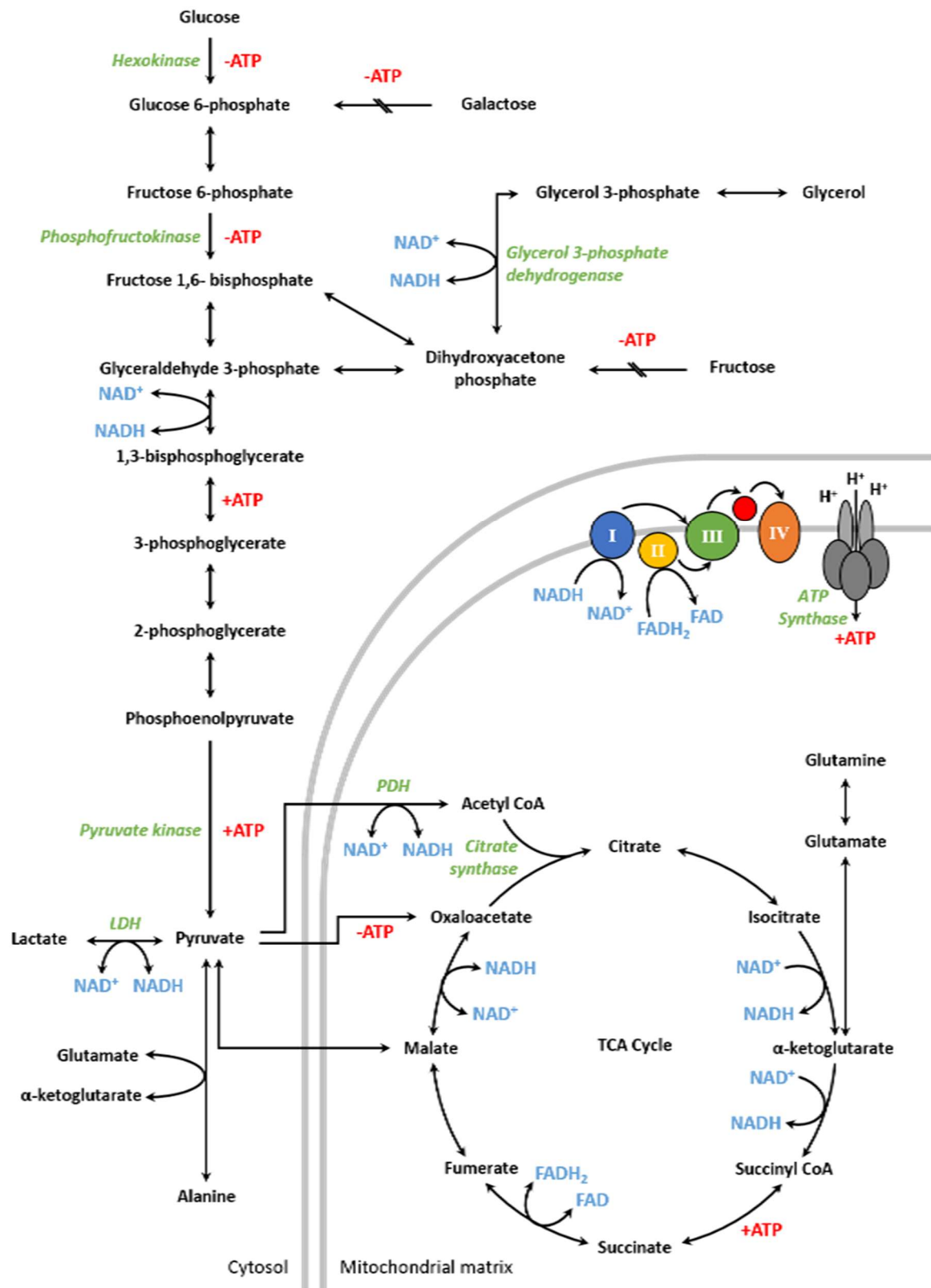


Figure 1 - Overview of glycolysis and the TCA cycle. Glucose is phosphorylated and enters the glycolytic pathway. It is broken down through a series of reactions into pyruvate, which can then enter the mitochondria to drive the TCA cycle. Reducing equivalents feed electrons into the ETC to generate a proton gradient. This proton motive force is used to provide energy for ATP synthesis.

move through the complexes of the ETC, releasing energy which is used to pump H^+ from the mitochondrial matrix into the intermembrane space. This results in a proton gradient across the inner mitochondrial membrane. Protons can then diffuse back down their electrochemical gradient into the matrix through ATP synthase. During this process, ADP is phosphorylated to ATP which is then used as a source of chemical energy for a wide range of cellular reactions. The terminal electron acceptor for electrons moving along the ETC is molecular oxygen, which is reduced to water. This process generates approximately 36 molecules of ATP per glucose molecule, so is significantly more efficient than anaerobic metabolism [3].

1.2 Metabolic Adaptation to the Extracellular Environment

Cells are sensitive to their surroundings and can adapt intracellular processes such as metabolic pathways to suit the extracellular environment. Detection of changes in the extracellular environment may occur at the cell surface through the action of receptors (e.g. insulin receptor [4]), or intracellularly, where molecular stimuli enter cells and cause direct effects (e.g. glucocorticoids [5]) [6].

A common example of environmental metabolic adaptation in prokaryotes is the use of the *lac* operon. Expression of β -galactosidase and β -galactoside permease (i.e. the enzyme which breaks down lactose into monosaccharides and the transporter which transports lactose into the cell) is driven by the lactose concentration and the presence of preferred sugars in the extracellular environment [7]. A repressor of the *lac* operon (*LacI*) is constitutively expressed and binds to the *lac* operator upstream of the operon. This prevents binding of RNA polymerase and therefore expression of the genes encoded within the operon. When lactose is present, it is

metabolised to allolactose which binds to the repressor protein. This prevents its binding to DNA and the operon becomes active, allowing the cell to import and metabolise lactose effectively. Expression is further enhanced in the absence of glucose. When glucose levels are low, cyclic AMP concentrations increase. Cyclic AMP binds to the catabolite activator protein (CAP) which itself binds to DNA upstream of the *lac* operon and supports the association of RNA polymerase with DNA [7]. Using this mechanism, the cells can respond to changes in available energy sources in their environment which enables survival.

In higher, multicellular organisms, the responses of cells within and between tissues may be co-ordinated using hormones. The maintenance of blood glucose homeostasis is a well-known example of this. Pancreatic β cells detect rises in blood glucose levels. Glucose enters the cells through the GLUT2 transporter and is metabolised by glucokinase, a specific type of hexokinase that has a lower affinity for glucose and does not undergo feedback inhibition by glucose 6-phosphate. This means the rate of glycolytic flux in these cells is more closely linked to the blood glucose concentration. Due to the low expression of LDH in pancreatic β cells [8], most pyruvate formed from glycolysis is directed into mitochondria and used to produce ATP. A change in the ATP/ADP ratio results in closure of ATP-dependent potassium channels. This depolarises the plasma membrane and voltage dependent calcium channels open. There is then an influx of Ca^{2+} into the cell which triggers the secretion of insulin through exocytosis [9]. In this way, the pancreatic β cells respond directly to glucose concentration, and the insulin they release co-ordinates a metabolic response to other tissues in the body.

Cells also respond to the extracellular environment by directly detecting nutrients [10]. Both AMP-activated protein kinase (AMPK) and the mammalian target of

rapamycin complex 1 (mTORC1) are key nutrient sensing proteins which allow the cells to detect nutrient levels and adapt cellular processes accordingly. AMPK is activated when ATP levels drop because there is a concurrent rise in AMP and ADP. This can occur under glucose limiting conditions [11]. AMP/ATP and ADP/ATP ratios allosterically control AMPK activation by enabling phosphatase access to a key residue on AMPK (T172 of the α subunit) [12]. When ATP is bound to AMPK, phosphatases can access this site and dephosphorylate the residue, inactivating the protein. When AMP or ADP bind, phosphatase access is inhibited and the residue remains phosphorylated, activating AMPK [12]. AMPK acts upon multiple metabolic pathways to preserve and produce ATP. To achieve this, AMPK upregulates glucose uptake and glycolysis, β -oxidation of fatty acids and autophagy while inhibiting protein synthesis, fatty acid synthesis and gluconeogenesis [12]. AMPK activation has also been suggested to increase mitochondrial biogenesis [13]. The effect of AMPK on protein synthesis is primarily conferred through mTORC1. mTORC1 promotes protein synthesis but AMPK phosphorylates the Raptor subunit of the complex and inhibits its activity [14]. Amino acid starvation also downregulates mTORC1 activity [11, 15]. 4EBP1 inhibits the eukaryotic translation initiation factor 4E (eIF4E), thereby preventing protein synthesis [16]. 4EBP1 is a target of mTORC1, which promotes protein synthesis by phosphorylating and deactivating 4EBP1 [15, 16]. In this sense, mTORC1 coordinates protein synthesis in response to both cellular amino acid and energy levels.

1.3 In Vitro Culture

The use of *in vitro* cell culture has exploded since the first immortal mammalian cells were isolated and cultured in 1951 [17]. These continuous cell lines allow experiments to take place without the use of animals or fresh human tissue samples. This limits ethical concerns and drastically reduces experimental costs, allowing faster scientific progress. However, it does not come without its issues. The translation of findings from an *in vitro* to an *in vivo* system is difficult, in part because the culture environment is vastly different to that found physiologically. Even in an *in vivo* system, the location of the cells can affect cell characteristics. This phenomenon was observed almost a century ago, where xenografts implanted into different locations (subcutaneously vs intraperitoneally) displayed different metabolic profiles [18].

The culture system differs from an *in vivo* environment in several ways. For example, a typical *in vitro* culture involves maintaining cells in a fixed body of medium whereas cells in the body are constantly perfused by the circulatory system. Perfusion cell culture systems have been developed with the aim to maintain a more stable extracellular environment, but these are often costly and technically challenging [19-21]. Such systems provide nutrients and remove waste products rapidly allowing the possibility of working under more physiological conditions. On the other hand, static cultures experience a decrease in nutrients over time while waste products accumulate. To prevent complete depletion of nutrients, most commercially available culture media contain such factors in excess. Additionally, most cells are cultured under atmospheric oxygen levels (~20%), whereas cells in the body are exposed to oxygen tensions of only a few percent [22].

1.3.1 Glucose

Glucose in culture media is often provided at a 25mM (4.5g/L) concentration. This is significantly above serum glucose concentration, which usually falls between 3.5 and 7mM [23]. This raises concerns with regards to the applicability of studies conducted in such media since the nutrient availability differs significantly from physiological levels and nutrient levels can affect cellular processes.

High glucose concentrations in culture have been found to cause an increase in reactive oxygen species (ROS) [24, 25] associated with mitochondrial fragmentation [26], and to inhibit AMPK independently of the AMP/ATP ratio [12]. Even transient high glucose has been shown to cause long term epigenetic changes [27]. Gene expression may be modulated by transcription factor activity directed by glucose. An example of this is the action of the carbohydrate responsive element binding protein (ChREBP). Under high glucose conditions, more glucose 6-phosphate is produced. This leads to higher flux through the pentose phosphate pathway, which runs parallel to glycolysis, and the amount of xyulose 5-phosphate in the cell increases. This activates protein phosphatase 2A which dephosphorylates ChREBP. ChREBP is now active and can relocate to the nucleus where it binds to DNA [28]. Here it can upregulate genes involved in glycolysis (e.g. L-type pyruvate kinase) and lipogenesis [10, 29]. This response is primarily active in liver and allows cells to respond to high blood glucose levels in an insulin independent manner [28].

Experiments which used siRNA to inhibit ChREBP expression showed that ChREBP downregulation was associated with increased mitochondrial oxidative activity [30]. Since ChREBP is inactive in cells cultured under low glucose conditions, this could explain why higher levels of OXPHOS are seen in these cultures. Conversely, high levels of glucose have been shown to suppress oxygen

consumption which could be explained by an increase in ChREBP activity [31, 32]. In a study by Potter et al. [31], cells cultured in 25mM glucose showed varying levels of extracellular acidification (indicative of glycolytic flux) and oxygen consumption. However, when the same cells were grown under low glucose conditions a shift occurred, with cells upregulating their oxygen consumption. This shows that the cells had the capacity to perform OXPHOS, but were not doing so when glucose was available in excess. Similar observations were made by Rossignol et al. [33] who found that HeLa cells had reduced OXPHOS in glucose compared to galactose. This phenomenon was first described in cancer cells by Crabtree in the 1920s and as such is termed the Crabtree effect [18, 34]. The Crabtree effect results in aerobic glycolysis, but is distinct from the Warburg effect in that it is conferred by short term mechanisms rather than long term reprogramming of metabolic pathways [34, 35]. The speed at which the Crabtree effect is implemented in cells suggests that it occurs as a direct response to stimuli rather than alterations in gene expression. The exact mechanism(s) that confers this is still under investigation, but a number of potential contributing factors have been suggested including mitochondrial outer membrane permeability and mitochondrial Ca^{2+} uptake [34-36]. Fructose 1,6-bisphosphate (F16BP), which is produced by phosphofructokinase during glycolysis, has been shown to accumulate in both yeast and tumour cells which are prone to the Crabtree effect. This metabolite has a suppressive effect on respiration conferred by inhibition of the ETC [36]. In contrast, the hexose monophosphates, glucose 6-phosphate and fructose 6-phosphate, slightly augmented respiratory activity [36]. This shows that intermediates in metabolism can act as 'metabolic messengers', but since all three of these metabolites are

products of glucose degradation and they exert opposing effects, regulation of glycolytic reactions themselves must also play a role.

This type of metabolic adaptation is also displayed by some species of yeast (e.g. *Saccharomyces cerevisiae*). *S. cerevisiae* will ferment glucose if it is freely available, but will switch to oxidative metabolism when only non-fermentable carbon sources are supplied [34]. This is an important survival mechanism for cells when substrate availability may change over time.

Alterations in metabolism such as these, which are mediated by cell culture conditions, have the potential to influence experimental outcomes. For example, studies assessing compounds which confer mitochondrial perturbations can be strongly affected by the Crabtree effect. If a mitochondrially active compound is added to cells in high glucose media, it may not cause any observable effects because the activity of mitochondria is already downregulated. Cells can meet their ATP requirements through glycolysis and so inhibition of mitochondrial function does not produce obvious effects. The same cells, under glucose limiting conditions, upregulate their OXPHOS to meet ATP demand which means they are more sensitive to compounds modulating mitochondrial function and differences can be observed [32]. Consequently, when screening for mitochondrially active compounds, choosing a suitable cell culture environment is of the utmost importance.

1.3.2 Glutamine

Glutamine is another important component of culture medium since it acts as a source of carbon and nitrogen. Despite glutamine being the most abundant amino acid in blood [37, 38], its concentration is still <1mM [39, 40]. However, it is typically

found in cell culture media at 2-4mM (DMEM = 4mM; DMEM/F12 = 2.5mM; RPMI = 2mM; MEM = 2mM; IMDM = 4mM). Glutamine has the potential to influence metabolism as it can drive anaplerotic reactions into the TCA cycle (see Figure 1). It can therefore drive oxygen consumption due to increased production of NADH/FADH₂. Furthermore, glutamine can be degraded in a process known as glutaminolysis. This pathway is often upregulated in cancers and involves the breakdown of glutamine into pyruvate/lactate and CO₂ [41].

Glutamine can affect gene expression resulting in a myriad of effects on cell function. For example, genes involved in lipogenesis are upregulated. This could reduce oxygen consumption by the mitochondria as acetyl CoA is diverted away to fatty acid synthesis. Phosphoenolpyruvate carboxykinase (PEPCK), a key gluconeogenic enzyme, is also upregulated under high glutamine conditions. The presence of supra-physiological glutamine levels (>5mM) antagonises the inhibitory effect of glucose on PEPCK expression [42], potentially increasing gluconeogenesis even in a glucose-rich environment.

1.3.3 Lactate

The accumulation of waste products in culture media can also influence cellular metabolism. Acidification of cell culture media often occurs and can be easily observed in media containing phenol red. This acidification is typically associated with lactic acid secretion. Lactate is excreted by cells through a monocarboxylate transporter along with a proton, thus export of lactate results in acidification of the culture medium. Both lactate itself and the influence it has on pH have the potential to affect cell growth and metabolism. Indeed, some cells have been shown to consume lactate and use this as a carbon source [43, 44]. In this sense, lactate can not only be considered a waste product, but also an alternative substrate. Its use as

a substrate has come under closer scrutiny in recent years due to its role in energy shuttling. In a process termed the reverse Warburg effect, cancer associated fibroblasts experience oxidative stress and switch to a glycolytic phenotype. The lactate these cells secrete is taken up by cancer cells which metabolise it as a fuel source [31]. A similar type of shuttling is also thought to occur between astrocytes and neurones, with astrocytes secreting lactate which is oxidised by neurones [45]. In addition to its use as a fuel, lactate can exert feedback inhibition on glycolysis [46] and influence the redox balance of the cytosol through the redox sensitive LDH catalysed reaction.

1.3.4 Serum

In vitro, serum is required by most mammalian cells for growth [47]. This is a problem as the serum added to culture medium is derived from animals and therefore there is a lack of consistency between batches. Serum collected over different continents and during different seasons can have a different composition [47]. This causes issues when comparing data obtained in different labs using different sources of serum. Most commercial suppliers test the sterility but not the composition of their product meaning it is difficult to determine how batch to batch variation may impact on experimental results. Researchers tend to only notice larger effects on cell growth or morphology with more subtle effects, such as those on cell metabolism, going undetected. There has been a growing effort to move towards serum free cell culture in both the interests of science and the reduction of animal use in research [48]. In particular, the biopharmaceutical industry utilises chemically defined media in the mass production of therapeutic proteins by mammalian cells. This is necessary to meet regulatory safety requirements as there is potential to pass contaminants (e.g. viruses, mycoplasmas, prions) through products of animal

origin [49]. Chinese Hamster Ovary (CHO) cells are used by the biotechnology industry and have been adapted to grow in a serum free environment for this reason.

Serum is a mixture of proteins (e.g. growth factors, albumin), hormones, lipids, vitamins and trace elements [47, 50] but its complexity and variability mean the exact composition of serum is unknown [49]. Furthermore, the composition of the commonly used foetal bovine serum (FBS) will differ from that of an adult human so may affect human-derived cell lines in a way that is not physiologically relevant. Not only does serum introduce unidentified variables into an experiment, but the wide range of components means it has the potential to drastically affect the phenotype of the cell, including its metabolic state. The following are all components of FBS which could modulate metabolism:

- i. **Insulin.** Insulin is found in FBS at approximately 10 μ U/mL [50] and most cultures cannot survive without it [47]. In adult humans, insulin is found at 8-11 μ U/mL between meals, however, after meals when blood glucose levels increase, insulin can peak at up to 60 μ U/mL [51]. Insulin enables glucose uptake by cells, stimulates glycolysis and increases the entry of substrates into the TCA cycle through the activation of pyruvate kinase and PDH. Insulin activates PDH indirectly, by activating PDH phosphatase, which removes inhibitory phosphate moieties from PDH. It also promotes transcription of the genes encoding hexokinase and pyruvate kinase, further enhancing glycolysis. Insulin also acts to reduce gluconeogenesis, glycogenolysis, lipolysis and proteolysis [4, 52].
- ii. **Transferrin.** Transferrin is found in serum and has a half-life of several days meaning it persists in culture [53]. It binds to ferric iron

(III) in serum and transports it into cells by receptor-mediated endocytosis. Transferrin bound to ferric iron (III) is endocytosed and the iron is subsequently released inside the cell when the pH inside the endosome is reduced [54, 55]. Iron is a necessary cofactor in multiple complexes of the mitochondrial ETC. For example, cytochrome c oxidase (complex IV) contains iron-containing haem groups, NADH dehydrogenase (complex I) and succinate dehydrogenase (complex II) contain iron-sulphur clusters while cytochrome bc₁ (complex III) has a combination of the two [56]. This means that iron transport into the cell is necessary for effective OXPHOS to take place. However, an excess of iron can also disrupt mitochondrial function [57] and since the ferrous (II) form of iron is highly reactive it can cause oxidative stress through the production of hydroxyl ions [58].

- iii. **Selenium.** Selenium is a trace element found in serum [59]. It protects cells against oxidative stress through its function as a cofactor in selenoproteins [60]. Glutathione peroxidase is a selenoprotein, most abundant in hepatic tissue [61, 62]. This enzyme catalyses the oxidation of glutathione and the concomitant conversion of hydrogen peroxide into water, thus protecting the cell against oxidative stress. NADPH is used to return glutathione to its reduced state. This, plus the fact that ROS can also act as redox signalling molecules [63], means that selenium could influence cell metabolism through modulation of the cellular redox state.

- iv. **Glucocorticoids**. This class of hormones, found in serum [47], typically have opposing effects to insulin. This means that they reduce glucose uptake and increase gluconeogenesis [64]. They have also been shown to inhibit β -oxidation of fatty acids in mitochondria [65]. Glucocorticoids bind to the intracellular glucocorticoid receptor and the complex acts as a transcription factor. A key gluconeogenic enzyme, PEPCK, is under glucocorticoid control [5]. Broadly, glucocorticoids act to preserve glucose in the extracellular environment.
- v. **Triiodothyronine**. The triiodothyronine hormone, also known as T_3 , upregulates mitochondrial gene expression, stimulates mitochondrial oxidative activity and increases adenine nuclear translocase (ANT) function [66]. Triiodothyronine was also found to improve coupling of glycolysis and oxidation in cardiac tissue [67].
- vi. **Lipids**. Lipids are found in serum as lipoproteins or as free fatty acids carried by albumin. Albumin is the major protein component of FBS [50] and binds to hydrophobic molecules to allow their transport through blood [68]. Fatty acids may be used in phospholipid synthesis or may undergo β -oxidation in the mitochondria to produce acetyl CoA and reducing equivalents which fuel the TCA cycle.
- vii. **Vitamin A**. Vitamin A is found in serum [59] and functions as an antioxidant [69]. Since ROS are important in redox balancing [70], they can affect metabolic pathways, of which many are dependent on redox state.

- viii. **Vitamin E**. Vitamin E is another vitamin found in serum [59] which also has antioxidant properties [71] and therefore can affect cell metabolism in a similar manner to vitamin A.

The above show how the presence of serum has the potential to interfere with metabolic studies. Slight concentration or batch to batch variations of serum can therefore impact experimental results.

1.3.5 Oxygen

The partial pressure of oxygen in the culture system can be manipulated. Some incubators allow control of oxygen levels, but often cells are simply cultured at atmospheric oxygen levels of ~20%. This results in comparable levels of oxygen in the culture medium. This is drastically different from tissue oxygen tension, which is typically only a few percent [22]. High oxygen tension leads to increased generation of ROS [72, 73] which damage macromolecular structures in cells and act as important signalling molecules [72, 74]. The generation of ROS can occur through a number of mechanisms, many associated with mitochondria and the ETC. Electrons leak from electron carriers such as those found in the ETC and reduce oxygen, forming superoxide or hydrogen peroxide [74]. The partial pressure of oxygen thus has the potential to affect ROS signalling cascades and metabolism. For example, atmospheric oxygen concentrations were shown to inhibit glucose uptake and glycolysis in neuronal cultures [72]. Because high levels of ROS damage cellular structures, the cell must carefully balance the presence of these molecules. Cells use antioxidants such as glutathione, vitamins A, E and C or enzymes such as superoxide dismutase to scavenge ROS. If the generation of ROS occurs more quickly than cells are able to scavenge it, oxidative stress occurs.

1.4 Aims

The aim of this project was to investigate ways in which the culture medium could influence the metabolism of CHO cells. Glucose, glutamine, lactate and serum levels were modified in the culture media and metabolic characteristics were assessed. To achieve this, two primary methods were used. First, the steady state level of ATP within cells was compared. Second, the oxygen consumption rate (OCR) was calculated. Oxygen is the final electron acceptor in the ETC so its consumption is indicative of electron flux through this system. In healthy mitochondria, this is closely linked to ATP production. Further information regarding the metabolic state of a cell can be obtained using metabolomics. This method uses mass spectrometry to collect data on small molecule metabolites found in a sample. This can provide a snapshot of the metabolite profile of the cell.

2. Materials and Methods

Unless otherwise stated, reagents were obtained from Sigma-Aldrich (St. Louis, MO, USA).

2.1 Culture of CHO cells

CHO cells were acquired from the American Type Culture Collection and were maintained in either GIBCO® DMEM (25mM D-glucose with pyruvate and sodium bicarbonate) supplemented with 10% (v/v) FBS, 50 units/ml penicillin and 50µg/ml streptomycin, 2mM L-glutamine and 0.6mM L-proline henceforth referred to as complete DMEM, or in GIBCO® Ham's F-12K (Kaighn's Modification) Nutrient Mix with either 10%, 1% or 0.1% (v/v) FBS at 37°C in humidified air plus 5% CO₂. Cells were passaged at approximately 80% confluency.

2.2 Seeding of CHO cells

For experiments investigating glucose, glutamine and lactate, cells were detached from the cell culture flask using a Trypsin-EDTA (0.5g/L porcine trypsin, 0.2g/L EDTA) solution, resuspended in complete DMEM and counted using a haemocytometer. Cells were seeded into flat bottom 96 well plates and left to adhere for at least 3 hours at 37°C in humidified air plus 5% CO₂. The media was aspirated and replaced with GIBCO® DMEM (no glucose, no glutamine, no phenol red) supplemented with 10% (v/v) FBS, 50 units/ml penicillin and 50µg/ml streptomycin, 0.6mM proline and the appropriate amount of D-glucose, L-glutamine or sodium lactate. Cells were incubated overnight (approximately 16 hours) at 37°C in humidified air plus 5% CO₂ in the relevant medium.

For serum concentration experiments, cells were pre-adapted to their respective FBS concentration for a minimum of 7 days. Cells were detached from cell culture

flasks using a Trypsin-EDTA (0.5g/L porcine trypsin, 0.2g/L EDTA) solution, resuspended in Ham's F-12K (Kaighn's Modification) Nutrient Mix supplemented with 10% (v/v) FBS and centrifuged at 1500rpm for 5 minutes. The cell pellet was resuspended in Ham's F-12K (Kaighn's Modification) Nutrient Mix containing 0.1% FBS and centrifuged again at 1500rpm for 5 minutes. The cell pellet was resuspended in Ham's F-12K (Kaighn's Modification) Nutrient Mix containing the appropriate concentration of FBS. Cell counts were made using a haemocytometer and cells were seeded into flat bottom 96 well plates and incubated overnight (approximately 16 hours) at 37°C in humidified air plus 5% CO₂.

2.3 Assessment of Cell Number using Hoechst

Cells which had been incubated overnight in a black, clear bottom, 96 well plate (Corning) were stained using a 1µg/mL solution of Hoechst 33342 and incubated at 37°C in humidified air plus 5% CO₂ for 25 minutes. The staining solution was aspirated and cells washed twice using 200µL of PBS. Fluorescence readings were obtained using a FLUOstar Optima plate reader (BMG Labtech) with the following wavelength settings: excitation 380nm; emission 460nm.

2.4 Assessment of Cell Death and Cell Number using Propidium Iodide (PI)

The media was aspirated from cells in a clear 96 well plate (Nunclon Delta Surface, Thermo Scientific) which had been incubated overnight at 37°C in humidified air plus 5% CO₂. 100µL of the appropriate medium was added along with 40µL of 175µM PI to give a final working concentration of 50µM. The cells were incubated with the PI for 30 minutes at 37°C in humidified air plus 5% CO₂. Fluorescence readings were obtained using a FLUOstar Optima plate reader (BMG Labtech) with the following settings: excitation 540nm; emission 620nm. Cells underwent x3 freeze (-80°C) thaw (37°C) cycles and fluorescence measurements were obtained

using the same settings. The first reading is representative of the number of dead cells, while the second reading represents the total number of cells. To calculate the number of viable cells, the first reading is subtracted from the second.

In the PI calibration experiment, a positive control was obtained by adding 4 μ L of Lysis Solution from a Promega CellTox™ Green Cytotoxicity Assay Kit to the staining solution.

2.5 Assessment of Total Cellular ATP

Cells were cultured overnight in a white (Corning) or clear (Nunclon Delta Surface, Thermo Scientific) 96 well plate and were assessed for relative ATP levels using the Abcam Luminescent ATP Detection Assay Kit (ab113849) according to the manufacturer's instructions. The culture medium was aspirated and replaced before the assay. A FLUOstar Optima plate reader (BMG Labtech) was used to measure luminescence. Standard curves were not constructed but results within an experiment are relative to one another and were normalised to cell number using readings obtained from either Hoechst or PI staining.

2.6 Assessment of Oxygen Consumption Rate (OCR)

OCRs were calculated for cells in a black, clear bottom 96 well plate (Corning) using MitoXpress® Xtra, an oxygen sensitive phosphorescent probe (Luxcel Biosciences). The lifetime signal of MitoXpress® Xtra is quenched by O₂, thus it can be used to indicate the concentration of molecular oxygen in a given solution. The kit was used as per manufacturer's instructions. In brief, media was aspirated and replaced with 140 μ L of the appropriate medium. 10 μ L reconstituted MitoXpress® Xtra was added to each well (except backgrounds) before high sensitivity mineral oil was applied. Fluorescence intensity was measured using a FLUOstar Omega

plate reader (BMG Labtech) with filter wavelengths of TR-exL 380nm for excitation and TR em2 615nm for emission. The temperature was set to 37°C. Time-resolved fluorescence (TR-F) with dual delay times of 30µs and 70µs, and 30µs integration times was measured. The TR-F was converted to phosphorescence lifetime values using the following equation:

$$\text{Lifetime } (\mu\text{s}) = \frac{D2-D1}{Ln \frac{W1}{W2}}$$

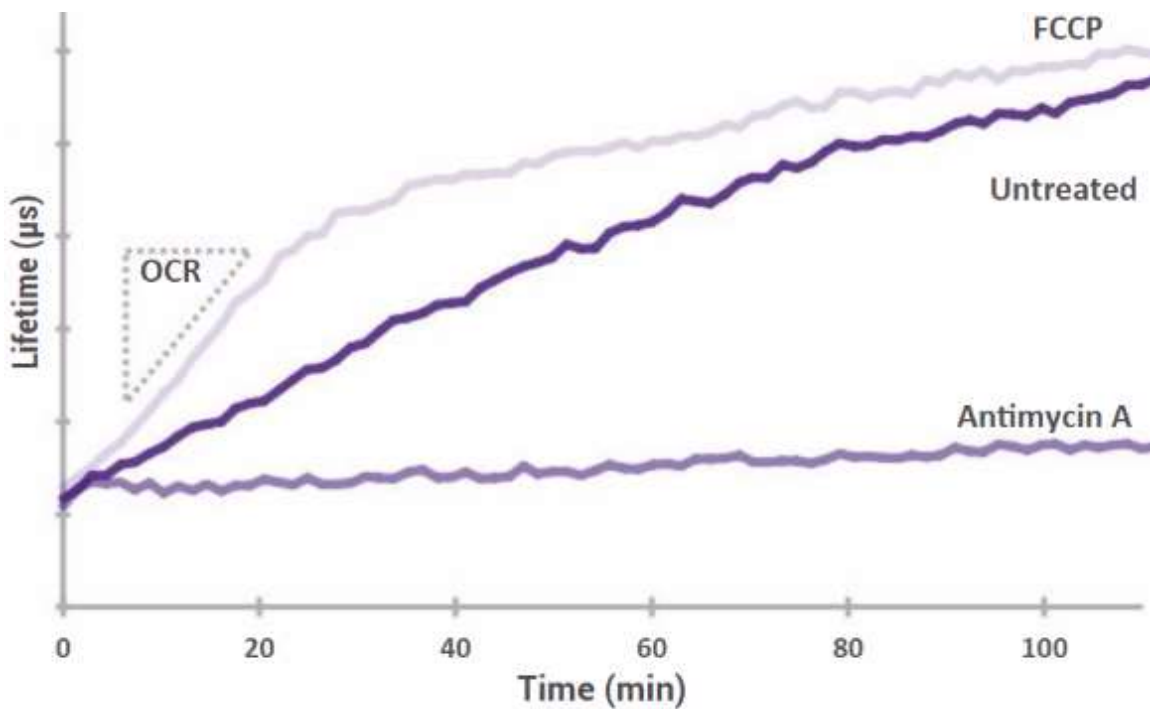


Figure 2 - Example plot showing fluorescence lifetime value against time.

The lifetime value of MitoXpress® Xtra is quenched by molecular oxygen. As oxygen is consumed by cells, the oxygen concentration in the medium decreases and the lifetime value increases. The addition of a mitochondrial ETC inhibitor, antimycin A, inhibits OXPHOS meaning oxygen is not consumed from the media and the lifetime remains low. FCCP is an uncoupler. It dissipates the mitochondrial membrane potential, forcing cells to upregulate flux through the ETC in an attempt to maintain a proton gradient. The OCR is increased under these conditions and this can be visualised and calculated by the increased gradient of the slope. Figure adapted from the MitoXpress® Xtra Oxygen Consumption Assay User Manual [1].

where D = time delay and W = measured intensity value. Once the lifetime value has been calculated, it can be plotted alongside time and the OCR can be calculated from the initial slope (see Figure 2). OCR results were normalised to cell number using readings obtained from either Hoechst or PI staining.

2.7 Growth Curve

1.5×10^5 cells were seeded into T25 tissue culture flasks and incubated for 3 hours at 37°C in humidified air plus 5% CO_2 . The media was aspirated and replaced with GIBCO® DMEM (no glucose, no glutamine, no phenol red) supplemented with 10% (v/v) FBS, 50 units/ml penicillin and $50\mu\text{g/ml}$ streptomycin, 0.6mM proline and the appropriate amount of D-glucose. At 24, 48, 72 and 96 hour time points, cells were detached from cell culture flasks using a Trypsin-EDTA (0.5g/L porcine trypsin, 0.2g/L EDTA) solution, resuspended in complete DMEM and counted using a haemocytometer. The total number of cells in each flask was calculated and used to construct a growth curve. Fresh medium was supplied every 24 hours.

2.8 Fluorescent Imaging

4-well ibidi μ -slides were coated with 0.1mg/mL poly-D-lysine before seeding with 4.9×10^4 cells in Ham's F-12K (Kaighn's Modification) Nutrient Mix with 10% (v/v) FBS. Cells were incubated overnight at 37°C in humidified air plus 5% CO_2 . Cells were stained using 200nM MitoTracker® Green FM (Invitrogen) and/or 200nM tetramethylrhodamine methyl ester (TMRM) (Life Technologies) for 40 minutes at 37°C in humidified air plus 5% CO_2 then washed x3 using PBS. Cells were maintained at 37°C in a heated chamber during imaging. Images were captured using a LEICA DMIRE2 microscope (40x objective) with Volocity software. MitoTracker® Green FM staining was captured using a FITC filter (excitation: 465-495nm; emission 515-555nm) and TMRM staining was captured using a TRITC

filter (excitation: 540/25nm; emission 605/55nm). Images were enhanced using ImageJ software.

2.9 Phase Contrast Imaging

CHO cells were pre-adapted in either 10%, 1% or 0.1% (v/v) FBS in Ham's F-12K (Kaighn's Modification) Nutrient Mix for at least 7 days before seeding into 100mm tissue culture dishes (Sarstedt) and incubating overnight at 37°C in humidified air plus 5% CO₂. Cells were imaged in these vessels using a Leitz Labovert FS phase contrast microscope (10x objective) with a QImaging Scientific CMOS camera attachment.

2.10 Metabolomics Sample Collection

CHO cells were pre-adapted in either 10%, 1% or 0.1% (v/v) FBS in Ham's F-12K (Kaighn's Modification) Nutrient Mix for at least 7 days before seeding into 100mm tissue culture dishes (Sarstedt) and incubating overnight at 37°C in humidified air plus 5% CO₂. To collect the samples, cells were rinsed twice in 5mL of PBS before addition of 500µL of ice cold methanol. After 2-3 minutes, the cells were scraped and the solution transferred to a 1.5mL Eppendorf tube. The lysate was centrifuged at 13000rpm for 30 minutes at 4°C. The resulting supernatants were filtered using Amicon® Ultra 10kDa molecular weight cut-off centrifugal filters (Merck Millipore) to remove any remaining soluble protein. Centrifugal filters were used as per manufacturer's instruction. Samples were normalised by addition of 80% methanol/water based on DNA content of the pellets collected below and transferred to Waters total recovery autosampler vials.

2.11 DNA Extraction and Quantification

DNA was extracted from pellets obtained using the metabolomics sample collection method described in Section 2.10 using the illustra Nucleon BACC2 Genomic DNA Extraction Kit (GE Life Sciences) and Proteinase K (Qiagen). Modifications to the manufacturer's protocol were made as described in Section 3.7. DNA was resuspended in 50 μ L of Tris-EDTA (TE) buffer and the quantity and quality was assessed using a NanoDrop Spectrophotometer ND-1000 to measure absorbance at 260nm (DNA), 230nm (purity) and 280nm (protein) wavelengths.

2.12 Metabolomics Liquid Chromatography and Mass Spectrometry

Samples were analysed by the Chemistry Research Lab, Oxford. Each sample was analysed using two different methods, one to identify amine based molecules and one to identify ionic/polar molecules.

To identify ionic and polar compounds, metabolite analyses were performed using a Thermo Scientific ICS-5000+ ion chromatography system coupled directly to a Q-Exactive HF Hybrid Quadrupole-Orbitrap mass spectrometer with a HESI II electrospray ionisation source (Thermo Scientific, San Jose, CA). The ICS-5000+ HPLC system incorporated an electrolytic anion generator (KOH) which was programmed to produce an OH⁻ gradient from 5-100mM over 37 minutes. An inline electrolytic suppressor removed the OH⁻ ions and cations from the post-column eluent prior to eluent delivery to the electrospray ion source of the MS system (Thermo Scientific QExactive-Orbitrap). A 10 μ L partial loop injection was used for all analyses and the chromatographic separation was performed using a Thermo Scientific Dionex IonPac AS11-HC 2 \times 250 mm, 4 μ m particle size column with a Dionex IonPac AG11-HC 4 μ m 2 \times 50 guard column inline. The IC flow rate was 0.250 mL/min. The total run time was 37 minutes and the OH⁻ gradient comprised as

follows: 0mins, 0mM; 1min, 0mM; 15mins, 60mM; 25mins, 100mM; 30mins, 100mM; 30.1mins, 0mM; 37mins, 0mM. Analysis was performed in negative ion mode using a mass scan range from 80-900m/z and resolution set to 70,000. The tune file source parameters were set as follows: sheath gas flow 60; aux gas flow 20; spray voltage 3.6KV; capillary temperature 320°C; S-lens RF value 70; heater temperature 450°C. AGC target was set to 1×10^6 and the Max IT value was 250ms. The column temperature was kept at 30°C throughout the experiment. Full scan data were acquired in continuum mode across the mass range m/z 60-900.

To identify amine based molecules, samples were analysed by derivatised LC/MS. Derivatisation of a 10uL aliquot of each extract was performed using a modified version of the Waters AccQ-Tag derivatisation method (Waters, Elstree, UK). C18 reversed-phase analysis of derivatised samples was performed using the Thermo Ultimate 3000 UHPLC system coupled directly to a Q-Exactive HF Hybrid Quadrupole-Orbitrap mass spectrometer. A 5µL partial loop injection was used for all analyses with pre- and post-injection wash program. A Waters AccQ-Tag column (2.1x100mm) was used with a flow rate of 0.5mL/min. The total run time was 9.5 mins. Mobile phase A and B comprised commercially available AccQ-Tag reagents prepared as recommended by Waters (Waters, Elstree, UK). The gradient elution program was modified from the published AccQ-Tag method as follows: 0mins, 0.1%B; 0.54min, 9.1%B; 5.74min, 21.2%B; 7.74mins, 59.6%B; 8.04min, 90%B; 8.05min, 90%B; 8.64min, 0%B; 9.5min, 0.1%B. The column temperature was kept at 40°C throughout the experiment. Mass spectrometry analysis was performed in positive ion mode using a mass scan range from 70-1050m/z and resolution set to 70,000. The tune file source parameters were set as follows: sheath gas flow 60 mL/min; aux gas flow 20 mL/min; spray voltage 3.6KV; capillary temperature 320°C;

S-lens RF value 70; heater temperature 350°C. AGC target was set to 1×10^6 ions and the Max IT value was 200ms. Full scan data were acquired in continuum mode.

2.13 Data Analysis

Statistical analysis of ATP levels, OCR and cell number was conducted using GraphPad Prism software. Significance and variance were tested using either a one- or two-way ANOVA. P values are denoted with asterisks ($p < 0.05 = *$, $p < 0.01 = **$, $p < 0.001 = ***$, $p < 0.0001 = ****$). On some figures, all significant results are labelled with a single asterisk for simplicity. In these instances, this is noted in the figure legend.

2.14 Metabolomics Data Analysis

Raw data was processed using Progenesis QI for small molecules (Waters, Elstree, UK). Briefly, this encompassed chromatographic peak alignment, isotope cluster recognition and compound identification. Identification of compounds in experimental samples was based on matching to an in-house library of authentic standards (Chemistry Research Laboratory, University of Oxford), using four measured parameters for each compound. These are: accurate mass measurement ($< 5\text{ppm}$) based on theoretical mass derived from the chemical formula; experimental retention time window of 0.3mins; an isotope pattern match (calculated from chemical formula) $> 90\%$; matching the fragmentation pattern with one from the analysis of an authentic standard of the compound, where these were available from survey scans. Statistical analysis was performed using Progenesis QI and the EZ info plugin for Progenesis QI developed by Umetrics. For each compound, the following were calculated: %CV (compounds with $> 30\%$ CV are excluded); p-value (significance < 0.05); Q-value; fold changes; mean abundance changes. The significance of binary comparisons is tested using Tukey's honest

significant difference (HSD) test. The difference in chemical composition of the samples was assessed using principle component analysis (PCA). Heat maps were generated manually.

3. Results

It is recommended that CHO cells are cultured in Ham's F12 medium. However, this medium is not available in glucose and glutamine free formulations, meaning experiments looking at the effect of these components would be difficult since the nutrients are already available in excess. For this reason, a stock of CHO cells was adapted to grow in DMEM. Proline was supplemented to 0.6mM as CHO cells are unable synthesise this amino acid. The cells were initially transferred to an equal Hams' F12 and DMEM mix and subsequently moved to complete DMEM cultures. There were no obvious phenotypic changes and the growth rates appeared comparable after the transition.

3.1 Determination of the Linear Range for Cell Number Assays

To normalise the results of metabolic experiments to cell number, fluorescence based assays were conducted on parallel plates. Initially, Hoechst staining was used as a surrogate for cell number. Hoechst is a fluorescent stain that binds to DNA, meaning fluorescence intensity is proportional to cell number. To confirm this, a calibration assay was conducted and the results show that the relationship between cell number and fluorescence is linear when 10,000-50,000 cells are seeded into a 96 well plate and incubated overnight (see Figure 3).

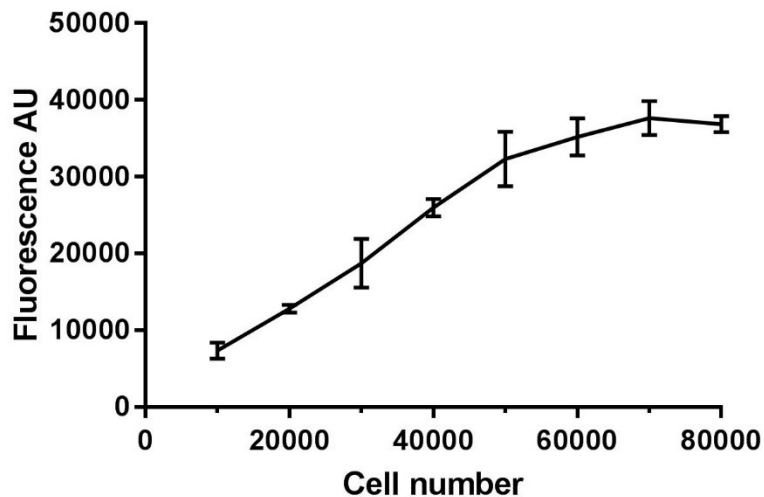


Figure 3 - Determination of linear range when using Hoechst as a marker for cell number. 10,000 to 80,000 cells were seeded into each well of a 96 well plate, incubated in 25mM glucose DMEM and stained with Hoechst after 24 hours (n=4). Fluorescence has a linear relationship with cell number if 10,000 to 50,000 cells are incubated overnight.

Propidium iodide (PI) is a DNA intercalating agent which undergoes an increase and shift in fluorescence when bound to DNA. However, this stain is non-permeant to living cells. This means it will selectively stain apoptotic/necrotic cells whose membrane integrity has been compromised. The stain is added to wells and a

reading is taken which is representative of the dead cell population. Cells undergo x3 freeze-thaw cycles and a second reading is taken which is indicative of the total cell number. A viable cell count can be achieved by subtracting the 'dead' cell reading from the 'total' cell reading. Figure 4 shows that the total cell reading is linear when 10,000-70,000 cells are seeded and incubated overnight. In control wells the dead cell read is consistent, showing background levels of fluorescence. Cells treated with lysis buffer show dead cell reads similar to those of total cells, showing that PI can give readouts for up to 100% cell death.

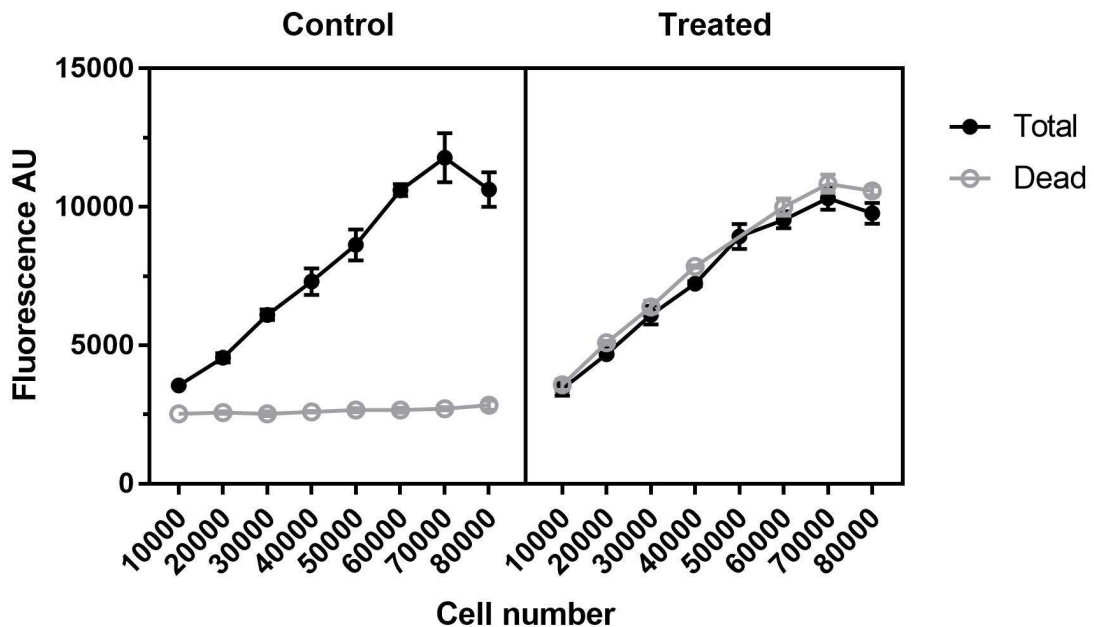


Figure 4 - Determination of linear range when using PI as a marker for viable cell number. 10,000 to 80,000 cells were seeded into each well of a 96 well plate, incubated in 25mM glucose DMEM and stained with PI after 24 hours (n=3). The total cell read is similar in both conditions and is linear from 10,000-70,000 cells. Cells treated with cell lysis buffer show high dead cell reads which are comparable to the total cell number. Control cells have a consistently low dead cell read showing high cell viability.

3.2 The Effect of Glucose on the Metabolic Profile of CHO cells

After CHO cells were adapted to grow in DMEM, experiments enforcing nutrient deprivation could be conducted. In the first instance, the effect of glucose on growth rate was assessed (see Figure 5). The growth curve showed that there was no significant difference in cell number after 24 hours at varying glucose concentrations, but that 1mM glucose medium reduced growth over a longer time period. Despite shorter incubations being used to gather experimental data, all experiments used parallel plates to normalise to cell number using the methods described above.

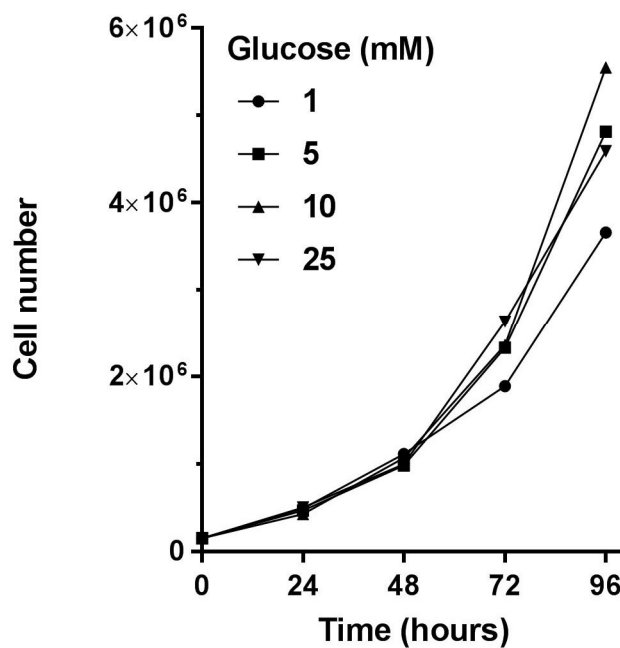


Figure 5 - Growth curve of CHO cells cultured in different glucose concentrations over 96 hours. There is no substantial change in cell number after 48 hours of culture. By 96 hours, the 1mM glucose medium has caused a decrease in cell growth, with approximately 1.5×10^6 fewer cells present.

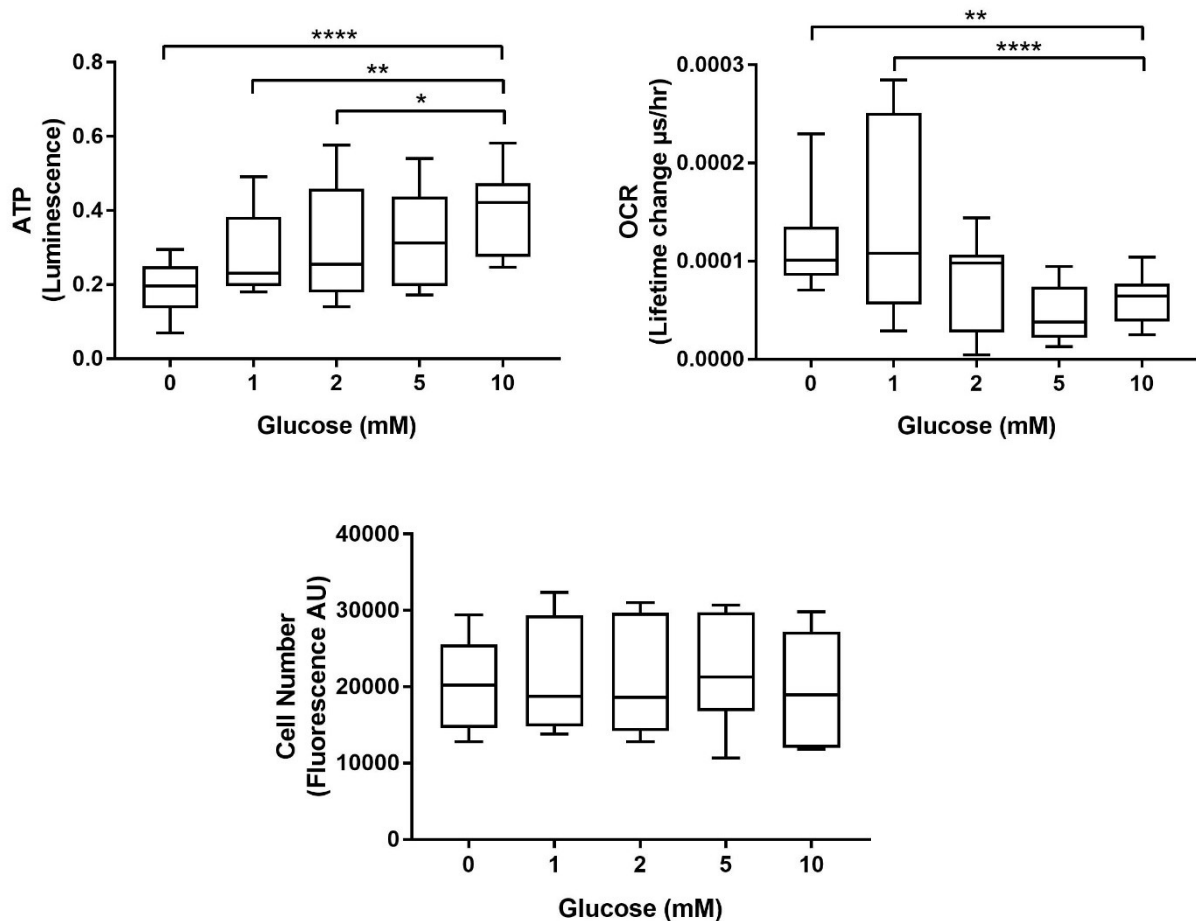


Figure 6 - The effect of glucose on ATP, OCR and cell number. Culturing cells in reduced glucose medium resulted in a decrease in ATP but an increase in OCR. No significant effect is seen on cell number. The culture medium contained 5mM glutamine. OCR and ATP values are normalised to cell number. Cells are cultured in their relevant medium overnight. The data presented were collected in three independent experiments and results were analysed using a two-way ANOVA.

Experiments consistently showed no significant difference in cell number under glucose deprivation conditions (see Figure 6). This is in agreement with the growth curve conducted using manual counting (see Figure 5). However, there were changes in the metabolic profile of these cells. Experiments showed changes in the level of intracellular steady state ATP, with a significant decrease in ATP levels in cultures containing low glucose (see Figure 6). There is a downward trend with ATP levels decreasing along with glucose concentration. Additionally, the OCR increased in cultures with low glucose. A significant increase in the OCR in the 0mM

($p = 0.0023$) and 1mM ($p < 0.0001$) conditions compared to the 10mM glucose condition is observed. This phenomenon has been previously reported [31]. It is suspected that cells in high glucose demonstrate the Crabtree effect and switch to generating ATP primarily through glycolysis, whereas cells cultured in lower concentrations of glucose must use their mitochondria to generate sufficient ATP, and therefore consume more oxygen through OXPHOS.

3.3 The Effect of Glutamine on Cell Metabolism under Various Glucose Concentrations

In order for cells in glucose deprived conditions to upregulate their OXPHOS, they require another source of carbon. As glutamine can feed into the TCA cycle via glutamate (see Figure 1), the effect of glutamine on cell metabolism was investigated. Cells cultured in various glutamine concentrations with excess glucose (10mM) showed a slight increase in ATP when glutamine was present at 5mM ($p = 0.0094$) but no significant differences in OCR (see Figure 7). The lack of a significant change in OCR suggests that glucose may be preferred over glutamine as a substrate in CHO cells.

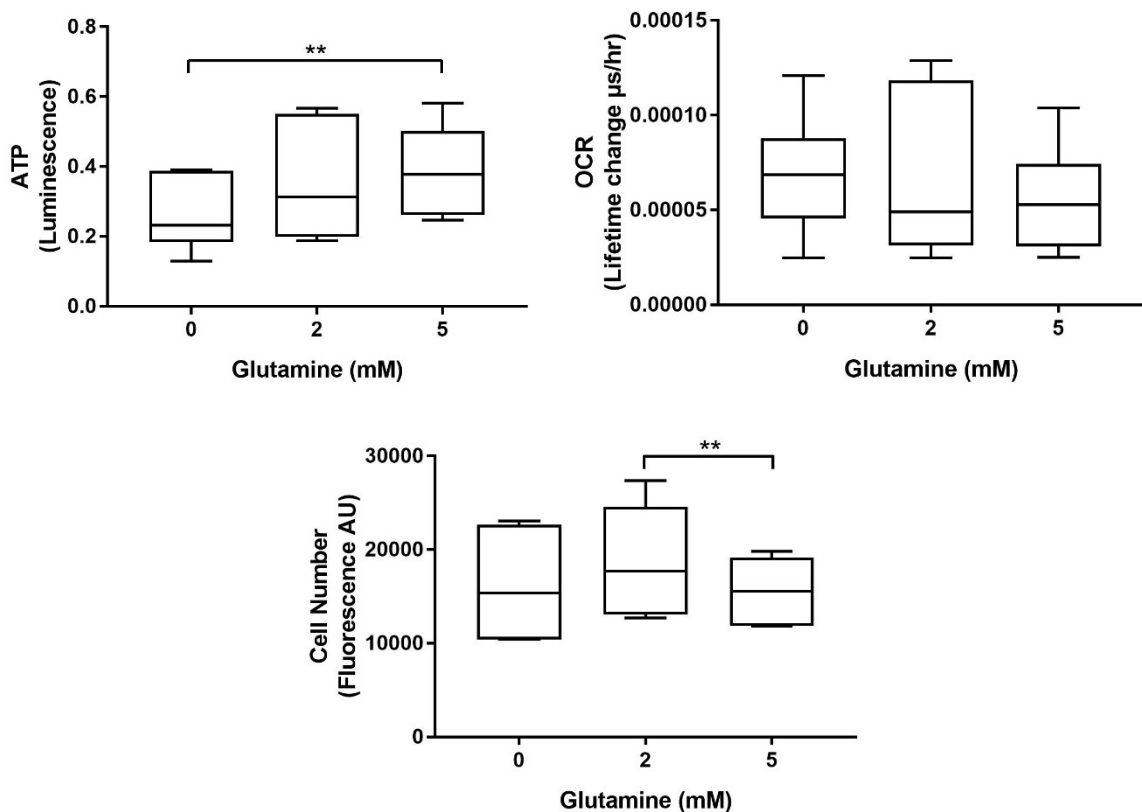


Figure 7 - The effect of glutamine on OCR, ATP and cell number in high glucose medium. There is no significant change in OCR but a decrease in ATP is observed when cells are glutamine deprived. The culture medium contained 10mM glucose and varying levels of glutamine. OCR and ATP values are normalised to cell number. Cells are cultured in their relevant medium overnight. The data were collected in two independent experiments and results were analysed using a two-way ANOVA.

It was hypothesised that glutamine would have a greater impact on cell metabolism when cells were also under glucose limiting conditions. This is because cells must switch to utilising alternative substrates such as glutamine when they cannot rely on glucose as an energy source. Although there was no significant effect on the ATP concentration with relation to changing glutamine levels, reducing the glucose concentration to 0mM and 1mM caused alterations in OCR to become apparent (see Figure 8). The OCR was significantly increased when glutamine was present. This supports the idea that glutamine is used to fuel the TCA cycle in the absence of glucose. There were also subtle but significant changes in cell number.

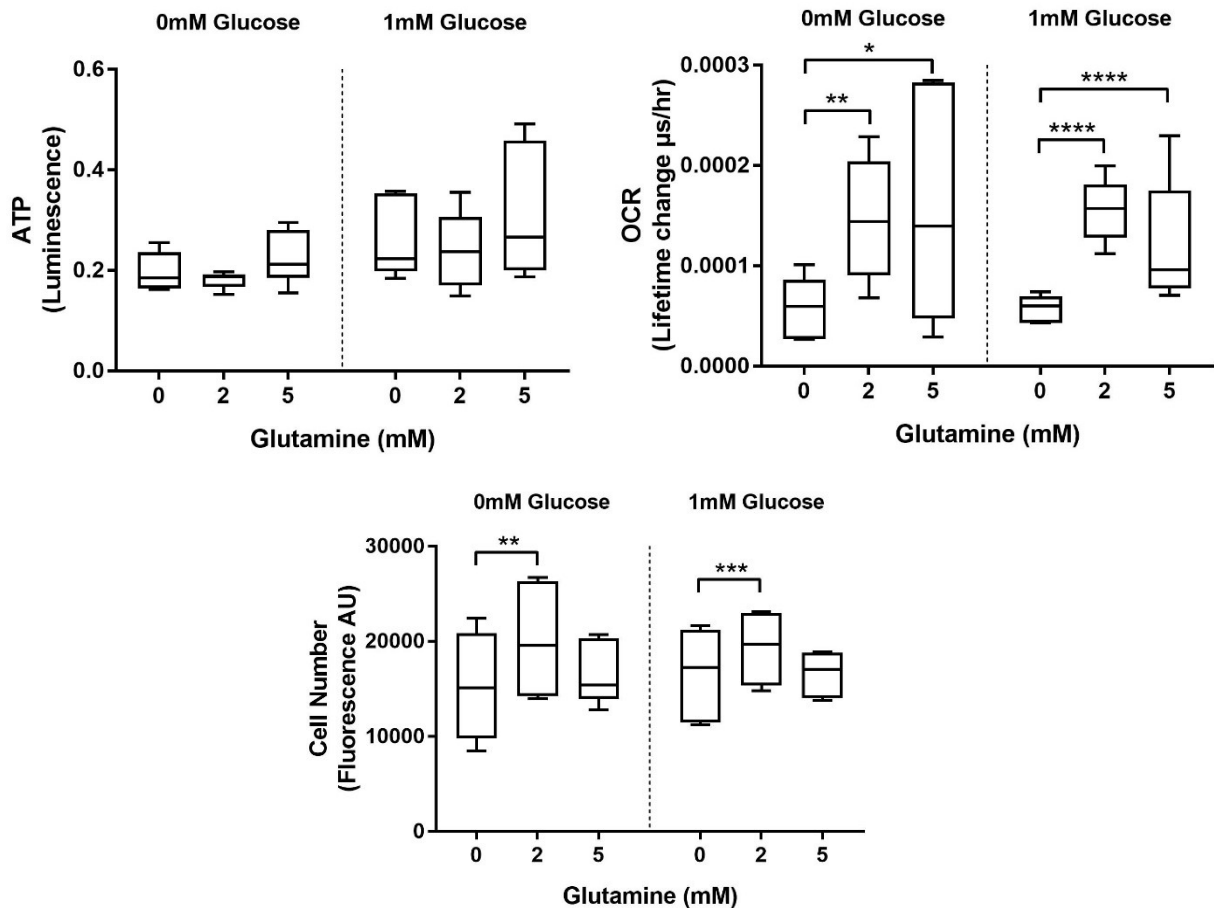


Figure 8 - The effect of glutamine on OCR, ATP and cell number under glucose limiting conditions. ATP levels remain constant, but there is a consistent increase in OCR across the three glutamine concentrations tested. Slight changes in cell number can be seen. OCR and ATP values are normalised to cell number. Cells are cultured in their relevant medium overnight. The data were collected in two independent experiments and results were analysed using a two-way ANOVA.

3.4 The Effect of Lactate on Cell Metabolism

Lactate is a waste product which frequently accumulates in cell culture media, particularly when cells are largely glycolytic. However, as it can also be used to produce pyruvate, its effect on metabolism was investigated here. Most importantly, it was found that the concentration of lactate did not affect viable cell number (see Figures 9 and 10). This suggests that concentrations of lactate up to at least 10mM

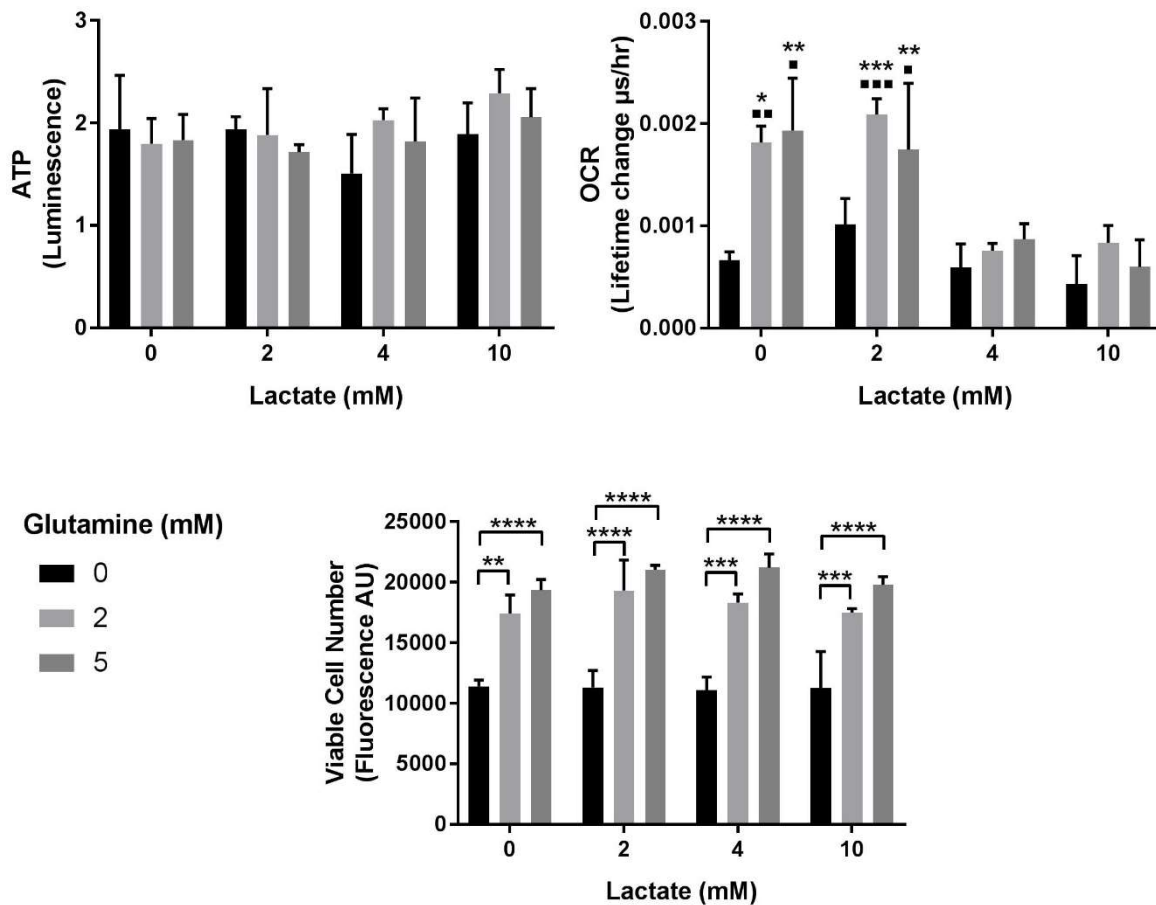


Figure 9 - Experiment 1 showing the effect of lactate and glutamine on ATP, OCR and cell number. Lactate had no significant effect on ATP or cell number, but did appear to suppress oxygen consumption at higher concentrations. Significance levels for OCR are shown compared to 4mM lactate (■) and compared to 10mM lactate (*) within the respective glutamine concentrations. Glutamine has a significant effect on cell number, and it is required for oxygen consumption at low lactate levels (significance bars not shown for simplicity). The culture medium here was glucose free. OCR and ATP values are normalised to cell number as measured using the PI stain. Cells are cultured in their relevant medium overnight. Data were analysed using a two-way ANOVA (n=3).

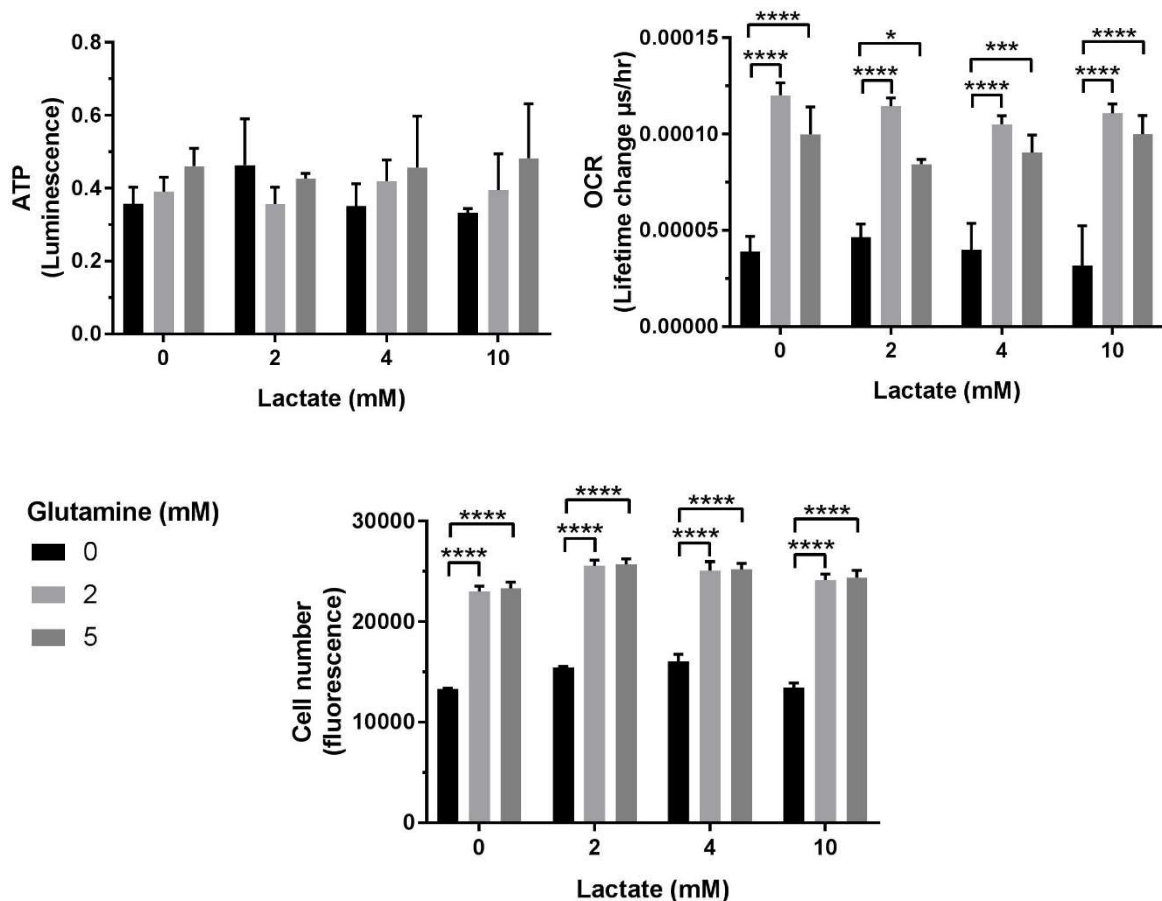


Figure 10 - Experiment 2 showing the effect of lactate and glutamine on ATP, OCR and cell number. Lactate had no significant effect on ATP, OCR or cell number. However, the presence of glutamine did have an effect. Glutamine increased both cell number and OCR. The culture medium here was glucose free. OCR and ATP values are normalised to cell number as measured using the PI stain. Cells are cultured in their relevant medium overnight. Data were analysed using a two-way ANOVA (n=3).

are well tolerated by CHO cells, as has been previously reported [75]. With regards to metabolism, ATP levels did not change in relation to the lactate concentration but conflicting OCR results were obtained. The first experiment (see Figure 9) shows lactate exerting an inhibitory effect on oxygen consumption in a similar manner to that of glucose. This is counterintuitive as lactate cannot be used to generate ATP through glycolysis, so it would be expected to feed into the TCA cycle and drive oxygen consumption. In the second experiment (see Figure 10), the suppressive

effect was not maintained, and the OCR across the various lactate concentrations was stable. The conflicting results found here mean the experiments would need to be repeated before any conclusions can be drawn. Under these conditions, glutamine had the largest effect, with glutamine deprivation reducing the OCR in both experiments (see Figures 9 and 10). Glutamine deprivation also had a larger effect on cell number when the cells were cultured in lactate rather than glucose. This is interesting as CHO cells express glutamine synthetase so should be able to produce the glutamine they need for growth. This points to the limiting effect of glutamine here being due to its use as an energy source rather than as a building block for proteins. It is also interesting to note that the ATP levels do not fall in cells cultured in 0mM glutamine, despite the fact there is no glucose present and the cells do not appear to be oxidising lactate.

3.5 Visualisation of CHO cells

Since a difference in metabolism can be accompanied/caused by a change in mitochondrial morphology, visualisation of CHO cells using mitochondrial stains was attempted. However, CHO cells do not flatten onto the surface as other cell types often do. This meant that imaging these cells using a microscope without confocal capabilities did not produce good results. Figure 11 shows a representative image of CHO cells co-stained with MitoTracker Green and TMRM. MitoTracker Green stains all mitochondria, whereas TMRM is loaded into mitochondria in a

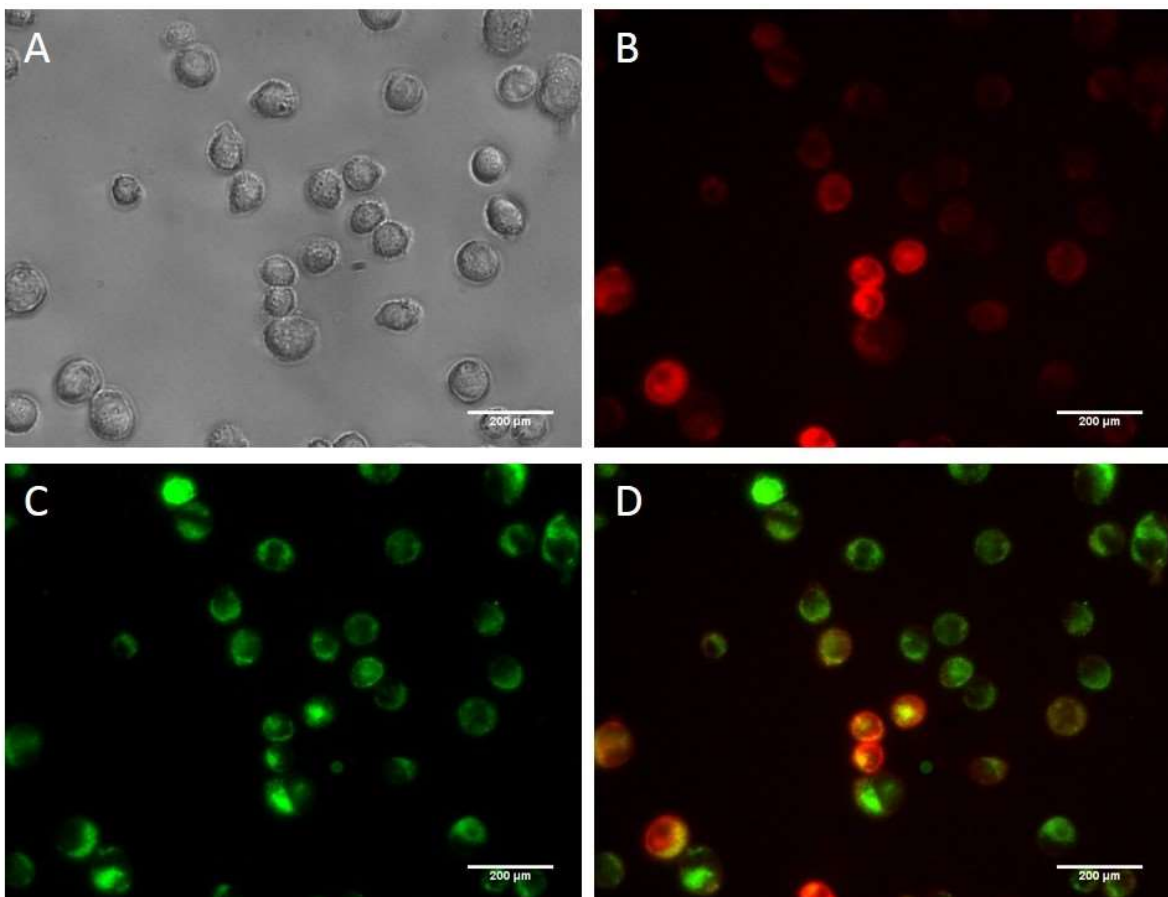


Figure 11 - Field of view showing CHO cells co-stained with MitoTracker Green and TMRM. (A) Bright field image. Cells appear small and rounded. **(B)** TMRM staining. No specific organelle structures can be seen. **(C)** MitoTracker Green staining. No specific organelle structures can be seen. **(D)** Overlay of TMRM and MitoTracker Green. MitoTracker Green appears to stain cells more consistently. Areas of overlap are shown in yellow. This occurs in fewer cells than expected.

membrane potential dependent manner. The images in Figure 11 show inconsistent TMRM staining with an unexpected lack of overlap between TMRM and MitoTracker Green. This could be indicative of low membrane potential in these CHO cells, but because no structural details can be seen it is difficult to draw any conclusions. There is also a large amount of variation in TMRM staining between cells, indicating variation in the mitochondrial membrane potential within the CHO cell population. Additionally, some cells are more strongly stained with MitoTracker Green. Since this stain is membrane potential independent, this could be indicative of differences in mitochondrial mass between cells. The images in Figure 12 show cells stained with MitoTracker Green. In image 12B, slight morphological details can be seen but these are poorly resolved. The technical difficulties encountered here prevented any further investigation into the mitochondrial morphology of CHO cells.

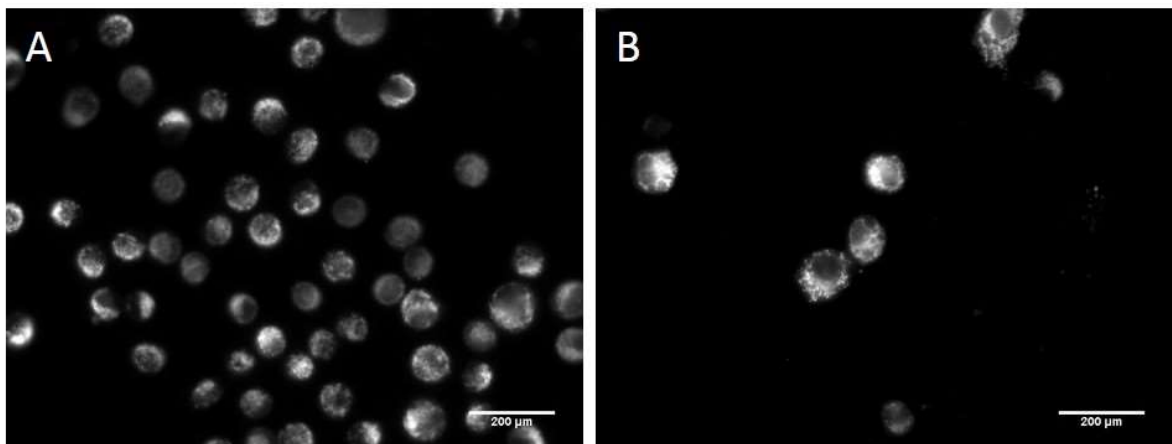


Figure 12 - CHO cells stained with MitoTracker Green. (A) A typical field of view with many CHO cells but poor resolution. In many cases, the staining appears brighter on one side of the cell. **(B)** Some individual mitochondria can be seen in this image at the periphery of the cell, but the resolution is poor.

3.6 The Effect of Serum on the Phenotype and Metabolic Profile of CHO cells

Serum is a major component of complete cell culture media but its effects on metabolism have not been extensively investigated. In this series of experiments, cells were adapted to grow under reduced serum conditions. 10% FBS was used as the standard control concentration, and the serum in the media was reduced by 10-fold (1% FBS) and 100-fold (0.1% FBS) before analysis. Firstly, there were obvious phenotypic changes which could be easily visualised using phase contrast microscopy at low magnification (see Figure 13). Compared to control cells, those in 1% FBS are indistinguishable, whereas those grown in 0.1% FBS have an elongated appearance, similar to that of fibroblasts. This cannot be accounted for by cell density as both cultures appear equally confluent.

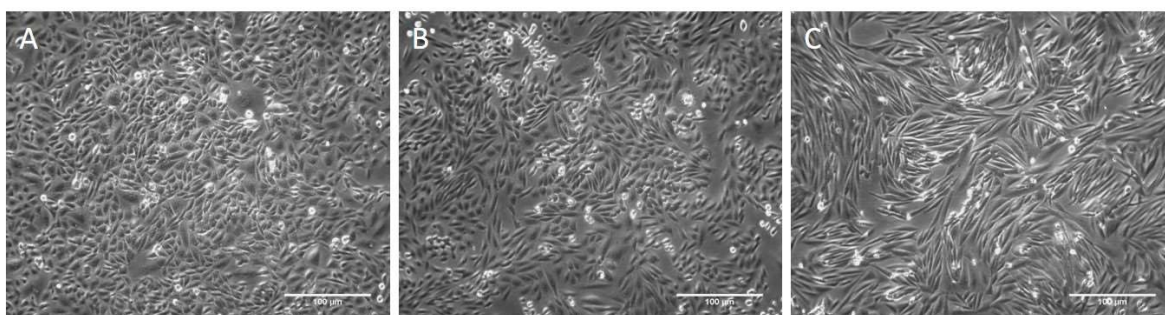


Figure 13 - CHO cells grown in varying serum concentrations and visualised using phase contrast microscopy. (A) CHO cells in the control conditions - 10% FBS. **(B)** CHO cells grown in 1% FBS. These appear comparable to control cells. **(C)** CHO cells grown in 0.1% FBS. Cells are elongated when compared to controls.

Following this, metabolic studies were conducted which showed significant differences in ATP levels and oxygen consumption associated with altered serum concentrations (see Figure 14). The concentration of ATP was significantly increased in the 0.1% FBS condition when compared to 10% FBS ($p = 0.0064$) and 1% FBS ($p = 0.0151$). The OCR was affected too, but showed a sharp, significant decrease when cells were reduced to 1% FBS ($P < 0.0001$) or 0.1% FBS

($P < 0.0001$). In addition, the growth and viability of these cells were affected to a greater extent than when carbon sources were altered. This is likely because serum provides multiple components which aid growth and affect cell health that cannot be easily replaced by other components in the culture medium. Both the total and viable cell number was reduced in the low serum conditions, indicating reduced growth. This is supported by observations during routine cell culture, as cells cultured in reduced serum required more time to reach confluency. There was also

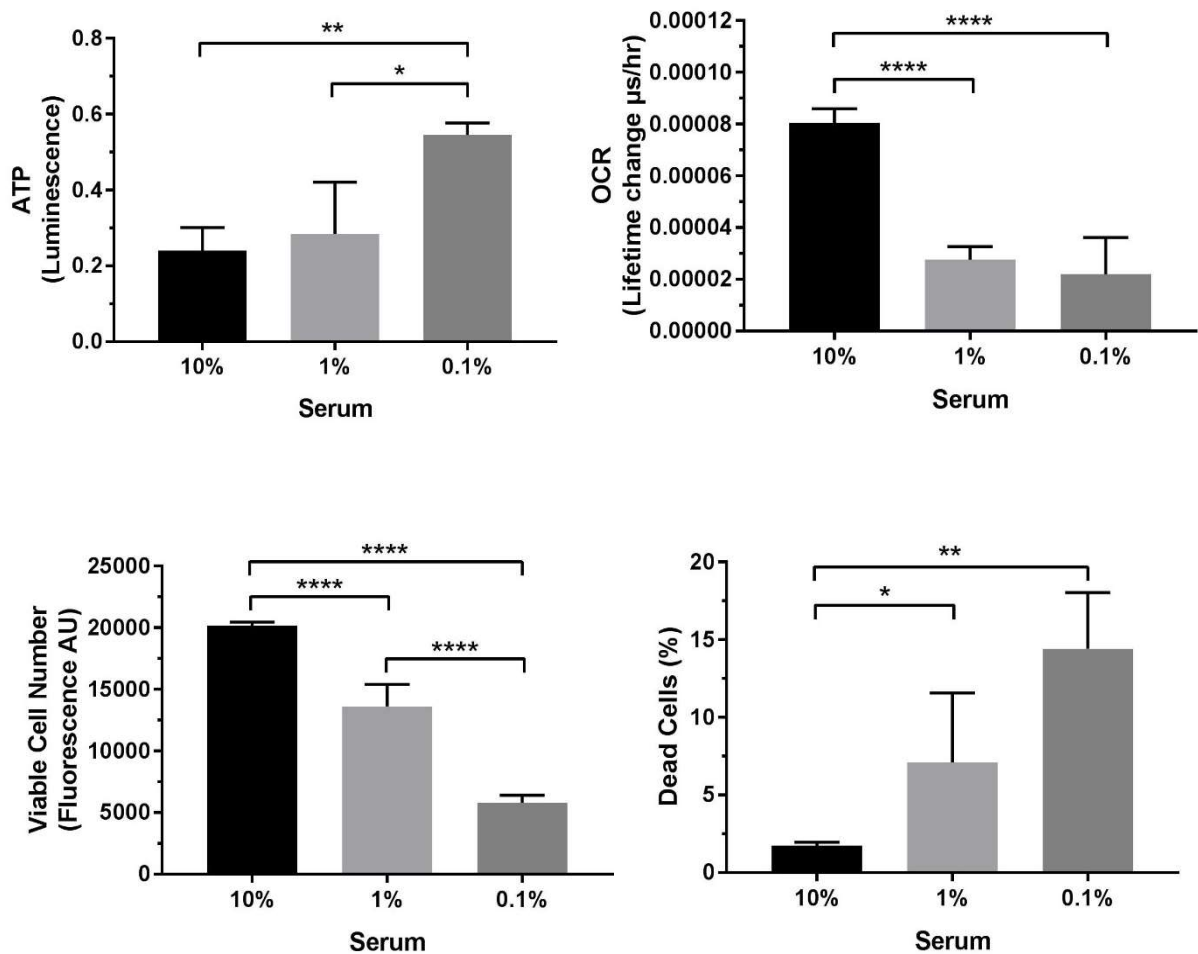


Figure 14 - The effect of varying serum concentrations on ATP, OCR, cell number and cell death. A decrease in serum resulted in increased ATP levels but a decreased OCR. The viable cell number also reduced in low serum conditions with a concurrent increase in cell death. OCR and ATP values are normalised to cell number as measured using the PI stain. Data were analysed using a one-way ANOVA ($n=4$).

a significant increase in cell death in the low serum conditions, cementing its importance for healthy cultures. Since serum conferred such a drastic change in cell metabolism, this component was selected for further analysis using metabolomics.

3.7 Extraction of DNA from Pellets Collected during Metabolite Extraction - Method Development

Typically, metabolomics samples derived from cell culture are normalised to cell number by plating and conducting a cell count on a parallel plate. This is problematic as the nature of the collection method for metabolomics samples means the proportion of cells collected can vary drastically. This will not be accounted for by a parallel plate where cells are trypsinised so the collection yield of cells is consistently high. Therefore, a new method for normalisation of metabolomics samples to cell number was developed.

Silva et al. [76] conducted an extensive study on various methods used to normalise metabolomics samples and found that DNA quantification obtained the best correlation with cell number over a large range. Furthermore, DNA could be quantified using the cell pellet which remains after metabolite extraction, removing the need for parallel cultures. However, the pellet which remains after metabolite extraction is more solid than a usual cell pellet due to its exposure to ice cold methanol. This means many DNA extraction kits cannot be used without modification.

Samples were collected as described in Section 2.10 and the illustra Nucleon BACC2 Genomic DNA Extraction Kit was used for DNA extraction. As the kit is designed to extract DNA from an untreated cell pellet, various modifications were attempted to improve DNA extraction. In Method 1, several attempts were made to dissolve the pellet. Reagent A was added and the pellet was vortexed and incubated for >30 minutes at 37°C but no change in the pellet was observed. The sample was centrifuged and Reagent A was replaced with Reagent B. Vortexing and incubation

Table 1 - Results of DNA quantification and quality assessment.

	Method 1		Method 2		Method 3	
	<i>High</i> 2 x 10 ⁶	<i>Low</i> 1 x 10 ⁶	<i>High</i> 1 x 10 ⁶	<i>Low</i> 0.5 x 10 ⁶	<i>High</i> 1 x 10 ⁶	<i>Low</i> 0.5 x 10 ⁶
DNA concentration (ng/ μ L)	521.4	341.9	454.9	115.4	431.6	250
260/280	1.79	1.83	1.95	2.06	1.97	1.98
260/230	1.13	1.16	2.05	2.26	2.21	2.25

at 37°C were again attempted, along with sonication but the pellet remained solid. Sodium perchlorate was added as per manufacturer's instructions. As the purpose of this step is deproteinisation, the incubation time was extended to overnight, as it was thought this step may aid disruption of the pellet. After overnight incubation on a rotary mixer, the pellet had broken into smaller fragments but fragments were still visible. The rest of protocol was followed as per the manufacturer's instructions. The results from this extraction are shown in Table 1. The presence of DNA, and the 1.52 ratio given by the relative high and low samples suggested that DNA quantification could be used as a surrogate marker. However, the low 260/230 ratio indicates the presence of various contaminants which absorb at 230nm such as carbohydrates or EDTA [77]. This indicated the purity of the extraction was poor, meaning some improvements had to be made.

Method 2 adhered more closely to the manufacturer's protocol, with the only modification being the incubation with Reagent B which was extended to overnight on a rotary mixer. This successfully dissolved the pellet and the rest of the extraction was conducted according to the manufacturer's instructions.

Method 3 was conducted as per the manufacturer's protocol but with one exception. An extra step was added after the resuspension in Reagent B but prior to the deproteinisation by sodium perchlorate step. 10µL of proteinase k was added to the samples, which were then incubated at 50°C for 2 hours. The results in Table 1 show improved 260/230 ratios for both Method 2 and Method 3 (i.e. closer to the expected 2.0-2.2 range). The ratio of the DNA yield between high and low samples were 3.94 and 1.72 for Methods 2 and 3 respectively. Method 3 was selected to assess DNA extraction in subsequent metabolomics experiments due to the improvement in both the total DNA yield and the high/low sample ratio, and the shortened extraction time.

3.8 Metabolomic Analysis of CHO cells in a Reduced Serum Environment

CHO cells grown in 10%, 1% and 0.1% FBS were collected and the cell contents analysed by mass spectrometry to produce a metabolite profile. The amount of cell extract analysed was normalised according to the DNA content of the pellets obtained using Method 3 described in Section 3.7. Two methods were used which suited quantification of amino acids (derivatised LC/MS, henceforth referred to as the 'amine method') and polar/ionic compounds such as those found in glycolysis and the TCA cycle (anion exchange chromatography/MS, henceforth referred to as the 'polar/ionic method'). An ANOVA test was used to calculate the significance of differences in the mean abundance of each identified compound across the three conditions (see Table 2). The data were also analysed to show fold changes and significance between binary groups within the three conditions (see Figures 15-20). In general, most changes were small (<5 fold), with the exception of taurine which was drastically increased in relation to serum concentration. The principle component analysis (PCA) plot based on compounds identified using the amine method shows the 10% FBS condition as a more distant group than 1% and 0.1% FBS (see Figure 21A). This shows that the 1% and 0.1% FBS samples are more similar to each other than each of them are to the 10% FBS samples. The lack of overlap between the conditions shows that the varying serum concentrations have caused distinct metabolite phenotypes to develop. The PCA analysis for the polar/ionic method shows the groups are less well separated, with the 1% FBS sample points falling between the 10% and 0.1% FBS samples (see Figure 21B). However, no overlap is shown between the groups, again demonstrating metabolic distinction.

There are certain striking results in this data set. For example, there appears to be an increase in TCA cycle intermediates in the 10% FBS sample, whereas glycolytic intermediates are increased in the 0.1% FBS sample (see Figure 22). However, this is not accompanied by an increase in lactate in the 0.1% FBS samples suggesting anaerobic respiration is not taking place. All amino acids shown in Figure 22 are increased in the 0.1% FBS condition. However, in general there is little change in the levels of proteinogenic amino acids (see Figure 23). The largest differences can be seen in aspartate and asparagine, which each showed a dose responsive decrease in concentration in relation to FBS supplementation.

Another important trend is the decrease in glutathione seen with increasing serum (see Figure 24A). Cells cultured in 0.1% FBS had significantly higher levels of reduced glutathione. This was dose responsive, with the average abundance of glutathione being 3.4x higher (abundance = 1,069,395) in 0.1% FBS, and 1.4x higher (abundance = 438,182) in 1% FBS compared to 10% FBS (abundance = 313,720). It is important to note that this value is representative of reduced glutathione only, and does not include the abundance of glutathione in its oxidised form since oxidised glutathione has a different molecular weight and structure. Many components surrounding glutathione synthesis are also affected (see Figure 25). In particular, the amino acids which contribute to glutathione synthesis are less abundant in the 10% FBS condition.

ATP was detected in the metabolomics samples but did not show the same trend as that detected by the luminescent assay used in Section 3.6 (see Figures 14 and 24B). In fact, the metabolomics data suggest that ATP was consistent across all three conditions. This brings into question the data collected in Section 3.6.

Table 2 - P values for the changes in metabolite abundance between 10%, 1% and 0.1% FBS cultures. Compounds in bold are significantly different ($p < 0.05$). 2-hydroxyglutarate, asparagine, citrate, sorbitol and taurine show the most significant changes.

Metabolite	P value	Metabolite	P value
2-Aminoadipate	0.144709	Histidine	0.657507
2-Deoxyadenosine triphosphate	0.007039	Inosine monophosphate	0.002828
2-Deoxyguanosine monophosphate	0.143694	Isobutylamine	0.037807
2-Hydroxybutyrate	0.001032	Isoleucine	0.497804
2-Hydroxyglutarate	<0.000001	Lactate	0.001459
a-ketoglutarate	0.000169	Leucine	0.022499
2-Phosphoglyceric acid	0.188332	Lysine	0.054463
Adenosine monophosphate	0.138721	Malate	0.128533
Adenosine triphosphate	0.464055	Mesaconic acid	0.050131
Adipate semialdehyde	0.043577	Methionine	0.021815
Alanine	0.37956	Methylglutaric acid	0.033464
Aminobutyrate	0.000951	N,N,N-Trimethyllysine	0.000143
Arginine	0.031373	N-Acetylneuraminic acid	0.000029
Asparagine	<0.000001	Pantothenic acid	0.000248
Aspartate	0.000053	Phenylalanine	0.021995
Citrate	<0.000001	Proline	0.193484
Creatinine	0.015514	Pyroglutamic acid	0.046297
Cytidine monophosphate N-acetylneuraminic acid	0.107978	Pyruvate	0.000064
Cytidine triphosphate	0.022194	Sarcosine	0.000001
Deoxycytidine triphosphate	0.000011	Serine	0.556378
Deoxyribose 5-phosphate	0.191972	Sorbitol	<0.000001
Deoxythymidine diphosphate-D-glucose	0.001467	Spermidine	0.087727
Ethanolamine	0.335205	Succinate	0.00012
Fructose 1,6-bisphosphate	0.033381	Succinate semialdehyde	0.000189
Fumarate	0.733689	Taurine	<0.000001
Glucose 1-phosphate	0.00604	Threonine	0.030602
Glucose 6-phosphate	0.060717	Thymidine triphosphate	0.006694
Glutamate	0.346404	Tryptophan	0.994927
Glutamine	0.000375	Tyrosine	0.796031
Glutathione	0.001372	Uridine diphosphate-gluconate	0.000081
Glycerol	0.036857	Uridine diphosphate-glucose	0.000331
Glycerol 3-phosphate	0.000015	Urea	0.172745
Glycine	0.01487	Uridine monophosphate	0.00237
Glycolic acid	0.102194	Uridine diphosphate-N-acetylglucosamine	0.004077
Guanosine monophosphate	0.039636	Uridine triphosphate	0.004341
Guanosine triphosphate	0.509275	Valine	0.268712

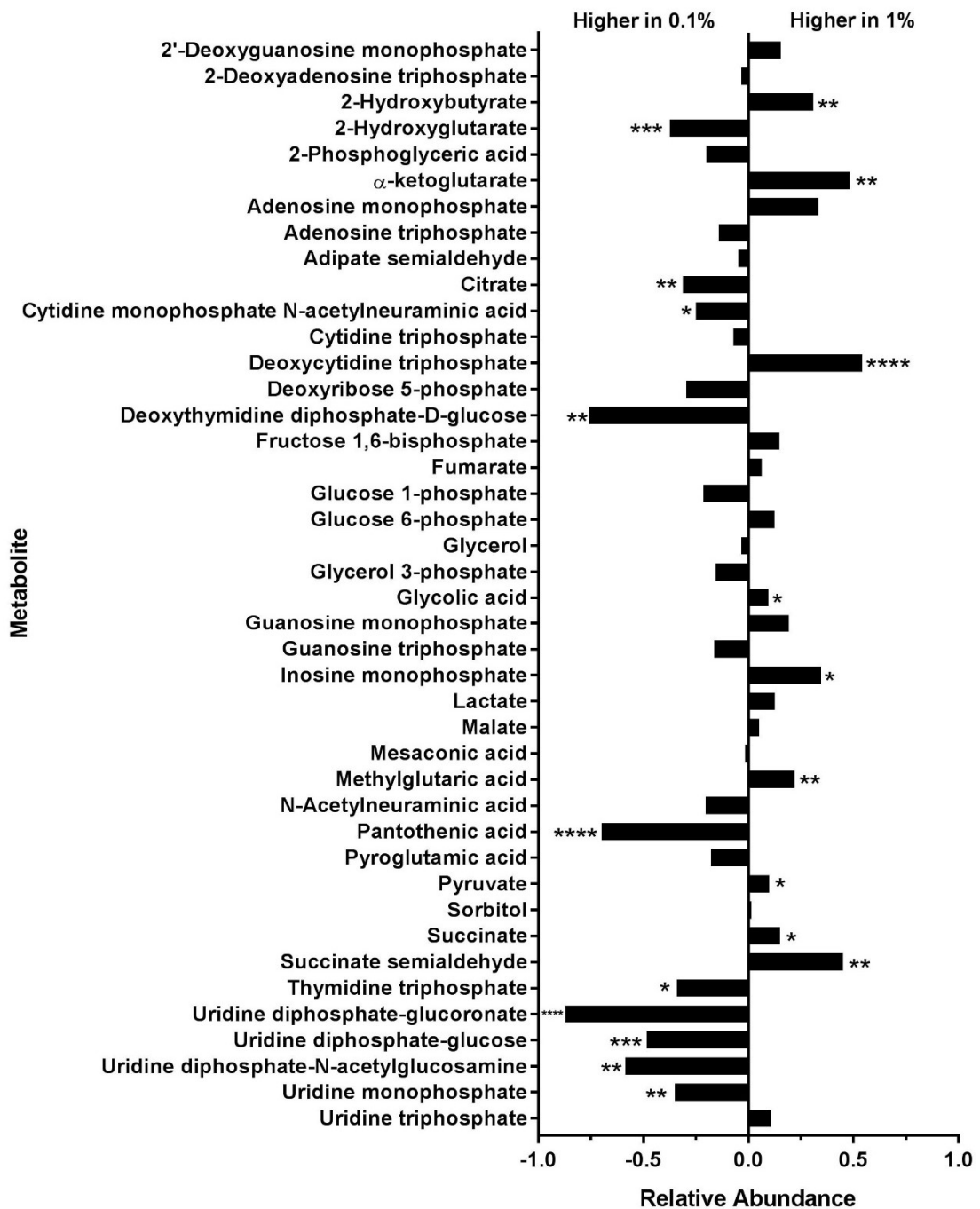


Figure 15 - The relative abundance of identified polar/ionic metabolites in cells from cultures containing 0.1% or 1% FBS. The relative changes in metabolite concentrations between these conditions are small. Deoxythymidine diphosphate-D-glucose, pantothenic acid and uridine diphosphate-glucuronate showed the biggest fold differences, all being more abundant in the 0.1% FBS condition. The most significant changes were seen in uridine diphosphate-glucuronate and deoxycytidine triphosphate.

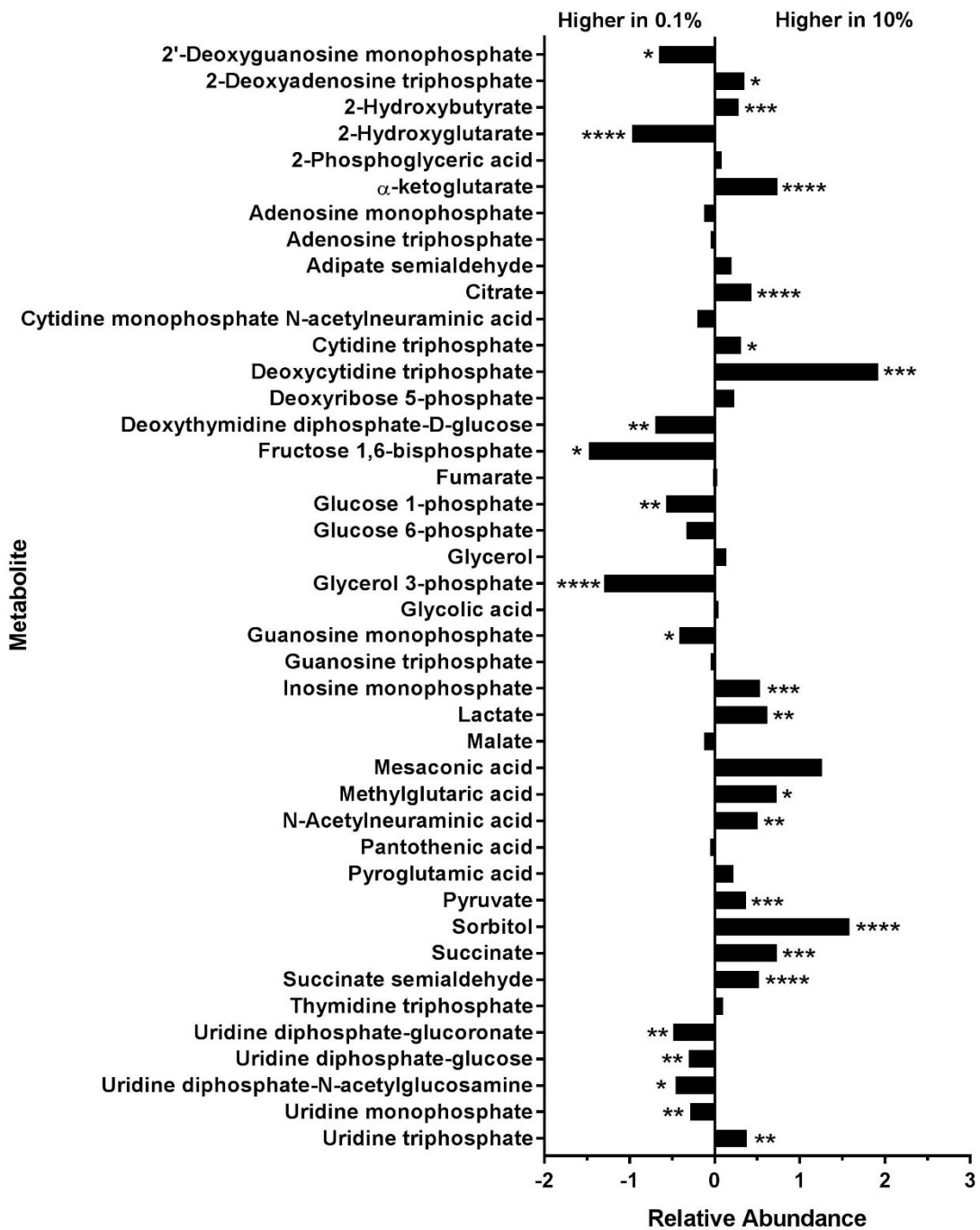


Figure 16 - The relative abundance of identified polar/ionic metabolites in cells from cultures containing 0.1% or 10% FBS. The relative changes in metabolite concentrations between these conditions are small, but larger than those seen comparing 0.1% and 1% FBS. Deoxycytidine triphosphate, fructose 1,6-bisphosphate, glycerol 3-phosphate and sorbitol showed the biggest fold differences. The most significant changes were seen in 2-hydroxyglutarate, α-ketoglutarate, citrate, glycerol 3-phosphate, sorbitol and succinate semialdehyde.



Figure 17 - The relative abundance of identified polar/ionic metabolites in cells from cultures containing 1% or 10% FBS. The relative changes in metabolite concentrations between these conditions are small, but larger than those seen comparing 0.1% and 1% FBS. Fructose 1,6-bisphosphate and sorbitol showed the biggest fold differences, with the most significant changes being observed in citrate, glycerol 3-phosphate, N-acetylneuraminic acid and sorbitol.

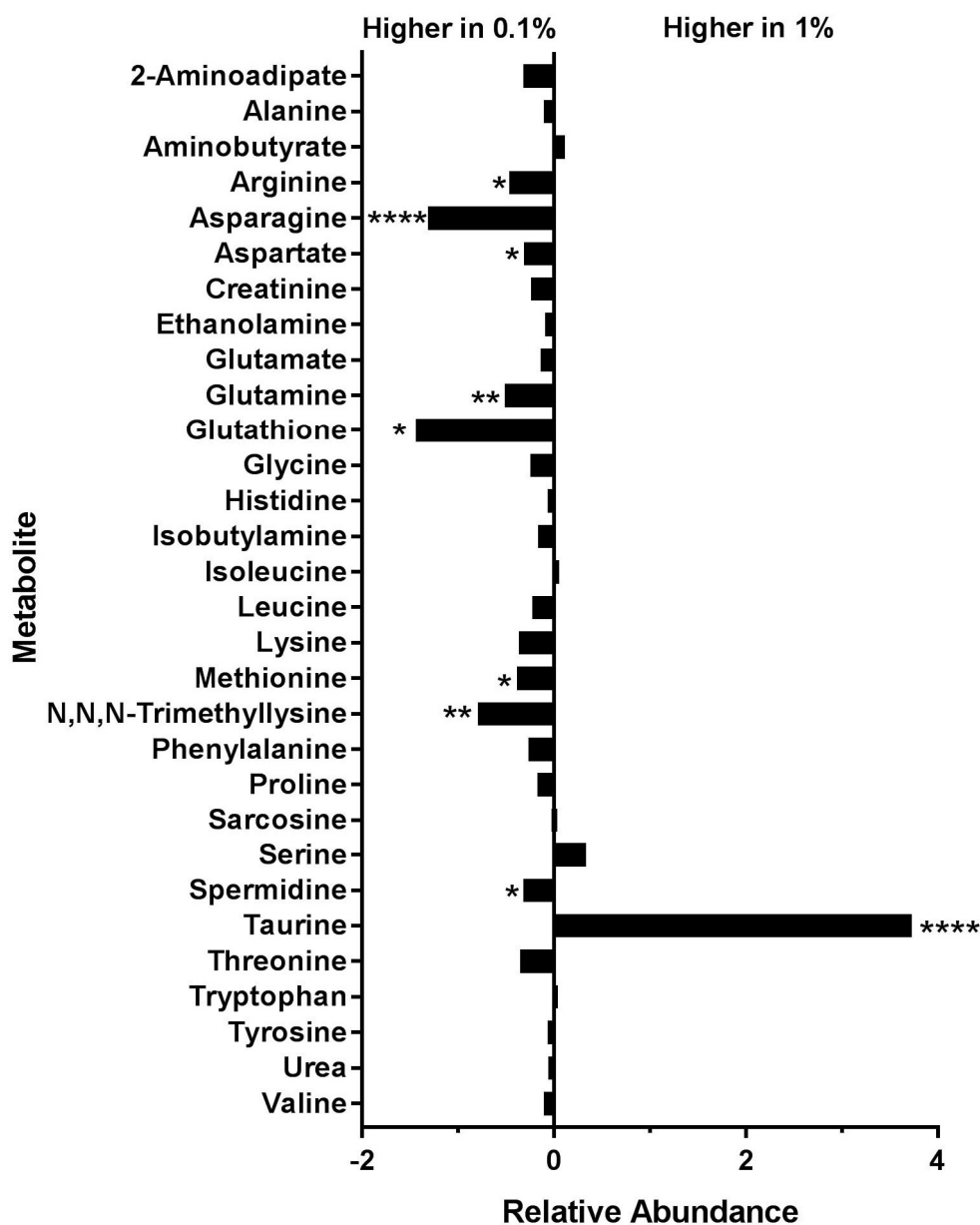


Figure 18 - The relative abundance of identified amine-based molecules in cells from cultures containing 0.1% or 1% FBS. The majority of amine based molecules were more abundant in the 0.1% FBS condition. The largest fold change was seen in taurine, with asparagine and glutathione also showing large changes. Accordingly, the most significant changes were seen in asparagine and taurine.

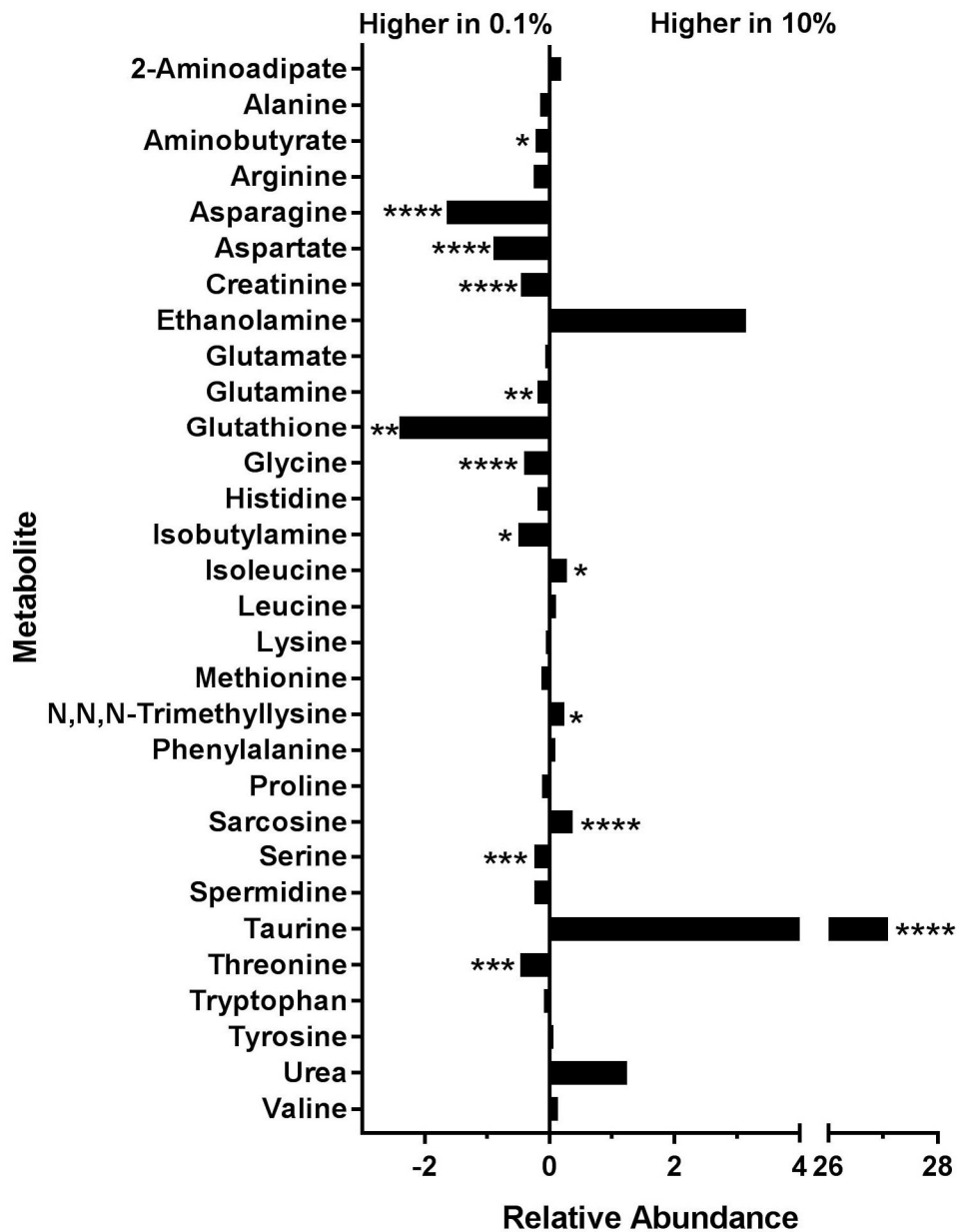


Figure 19 - The relative abundance of identified amine-based molecules in cells from cultures containing 0.1% or 10% FBS. By far the largest fold change was seen in taurine, with asparagine and glutathione also showing large changes. The most significant changes were seen in asparagine, aspartate, creatinine, glycine, sarcosine and taurine.

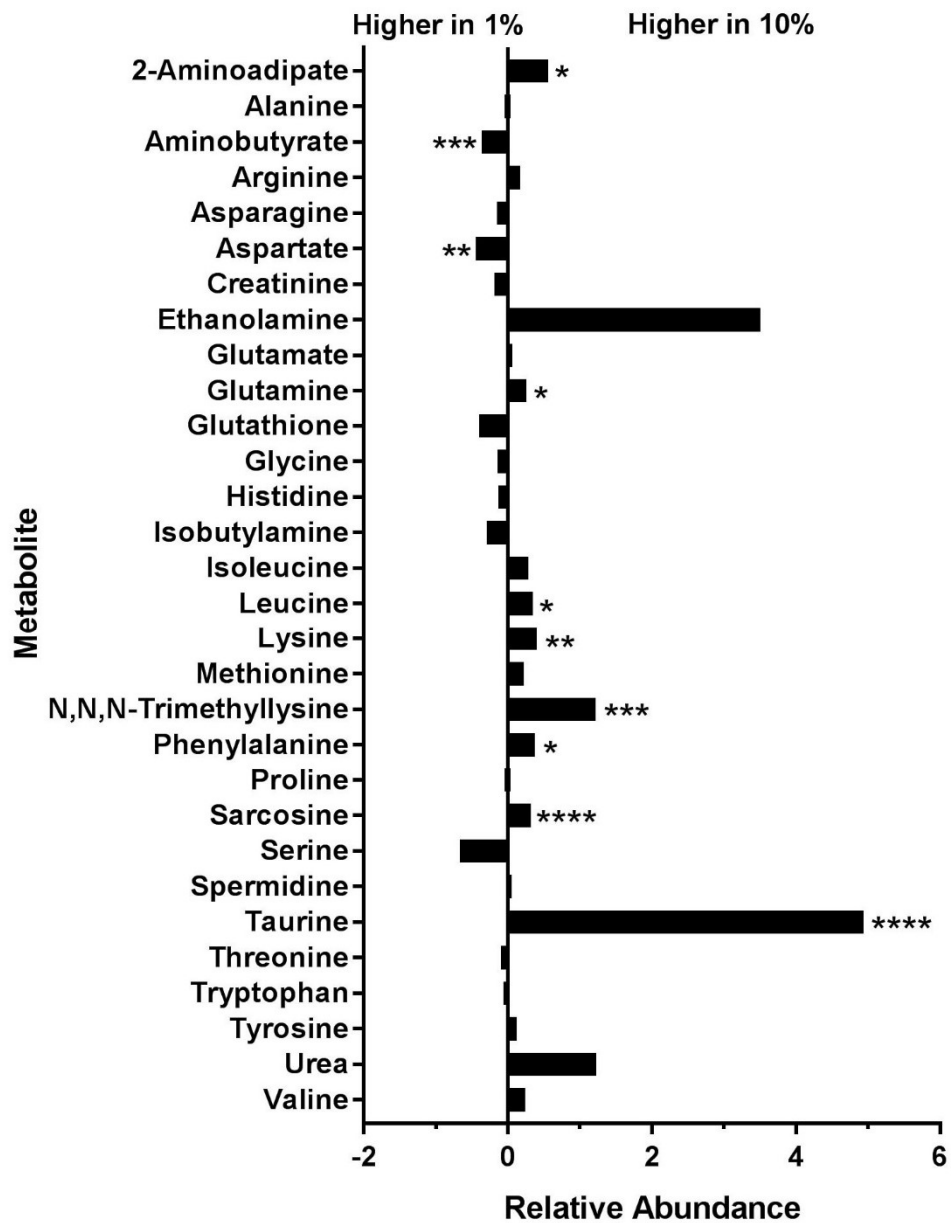


Figure 20 - The relative abundance of identified amine-based molecules in cells from cultures containing 1% or 10% serum. The largest fold change was seen in taurine. Taurine and sarcosine showed the most significant changes in this comparison.

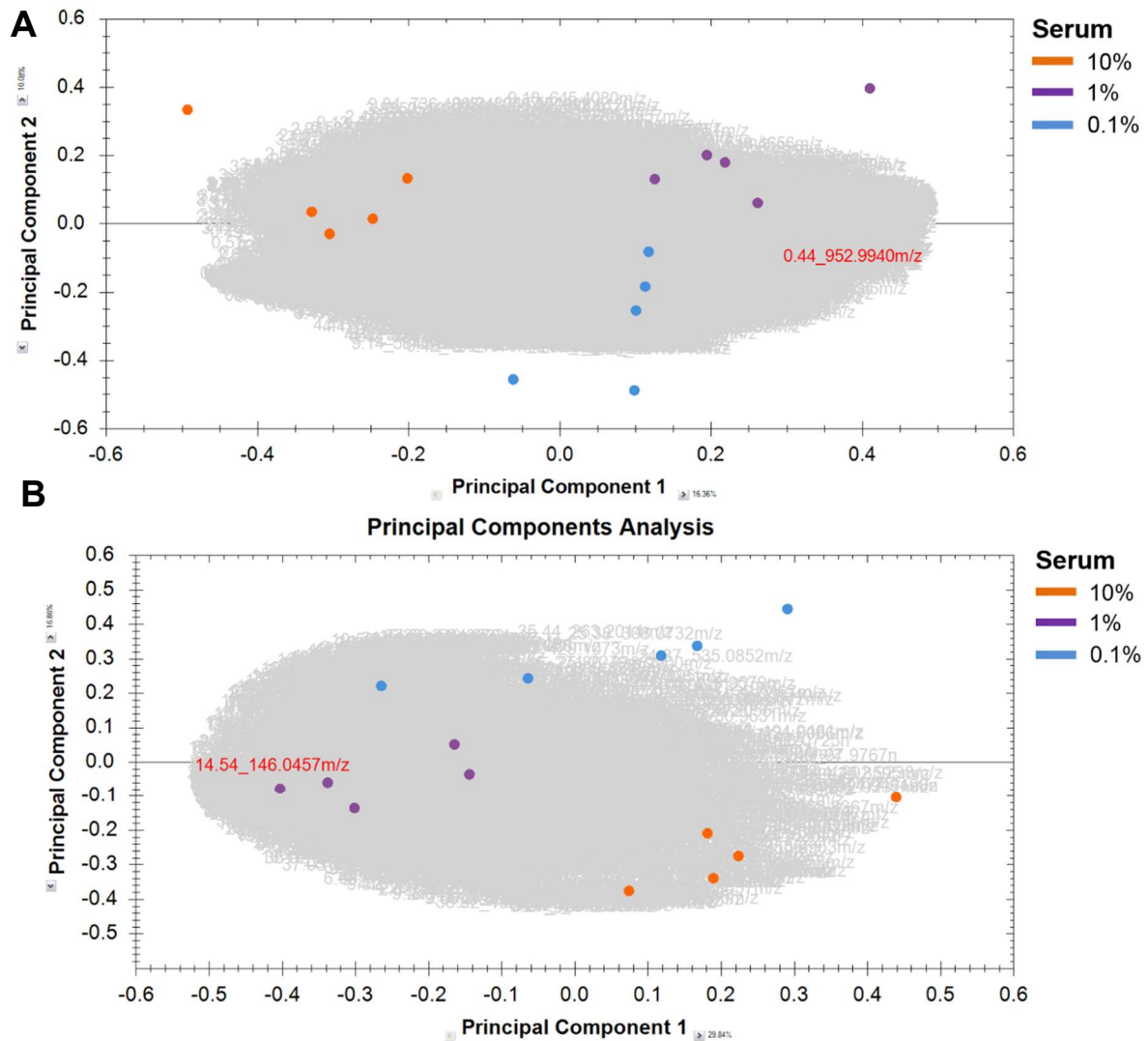


Figure 21 - PCA of the metabolite profiles of 10%, 1% and 0.1% FBS cultures. (A) PCA of the results using the amine method. Samples from each experimental condition are well separated. The 10% FBS sample is more distant than the two low serum conditions, indicating a more distinct metabolic phenotype. There are a small number of outliers but most samples shown an expected amount of variation. (B) PCA of results obtained using the polar/ionic method. There is no overlap between groups, but the separation is less distinct than that shown in A. The 10% FBS and 0.1% FBS samples have the greatest distance between them, showing they have the most distinct metabolite profiles.

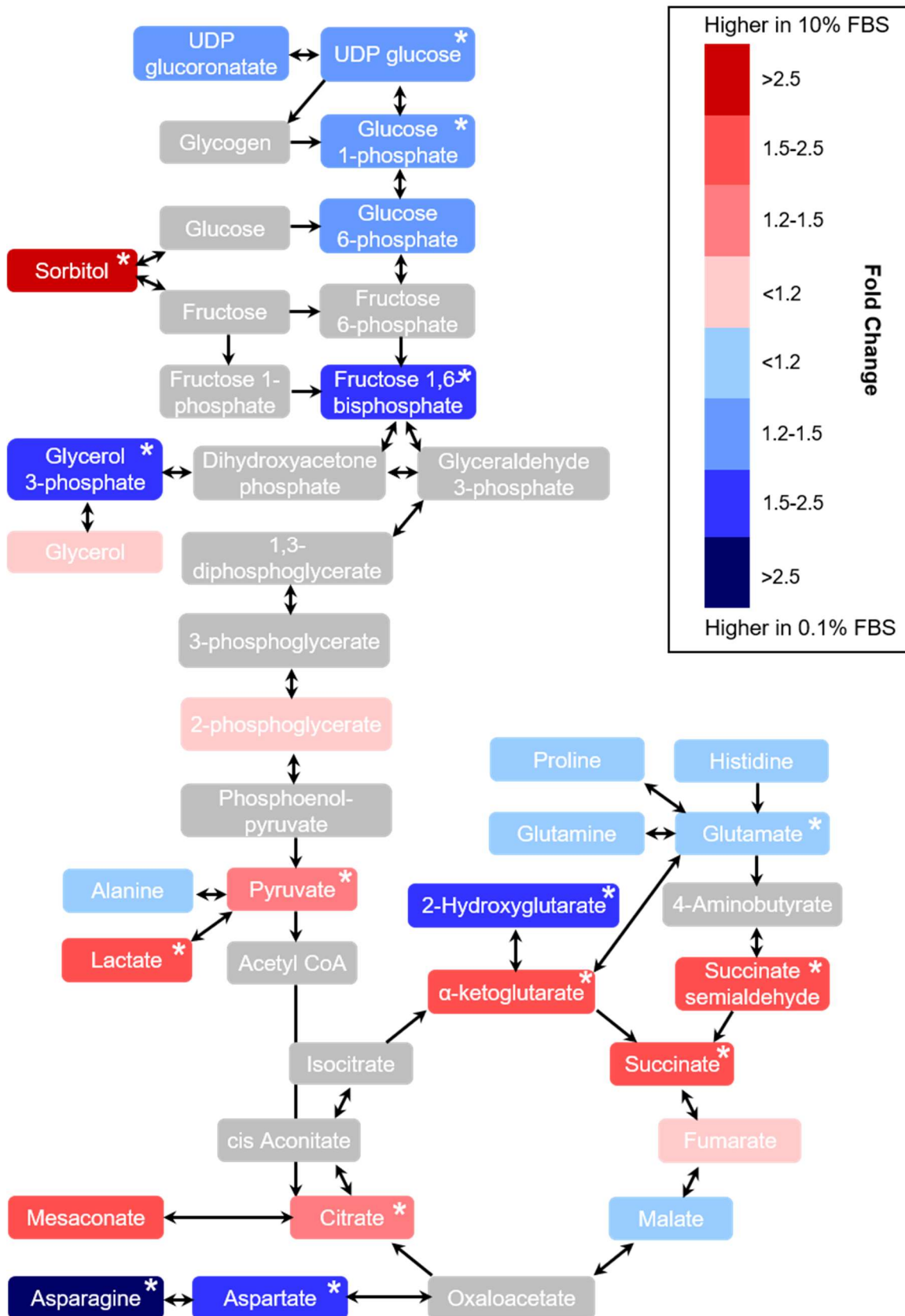


Figure 22 - Glycolysis, the TCA cycle and related intermediates: fold changes in 10% vs 0.1% FBS cultures. Fold change is indicated by the colour of the boxes. All metabolites which changed significantly ($p < 0.05$) between these two conditions are denoted with a single asterisk. Compounds in grey boxes were not identified.

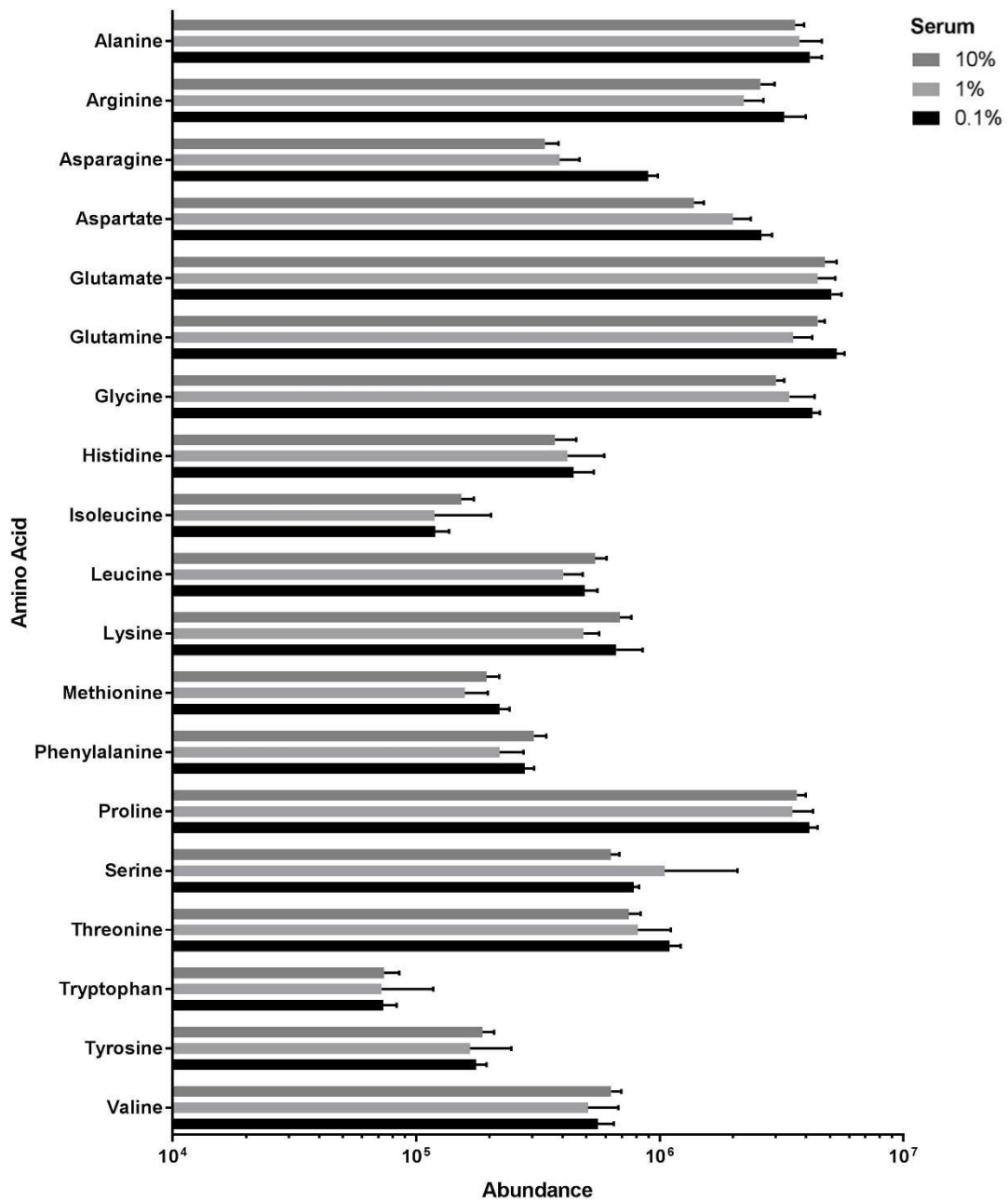


Figure 23 - The abundance of proteinogenic amino acids. All proteinogenic amino acids were detected with the exception of cysteine. Generally, the abundance across the three conditions is stable. The largest differences are seen in asparagine and aspartate. Data are shown on a log scale for clarity.

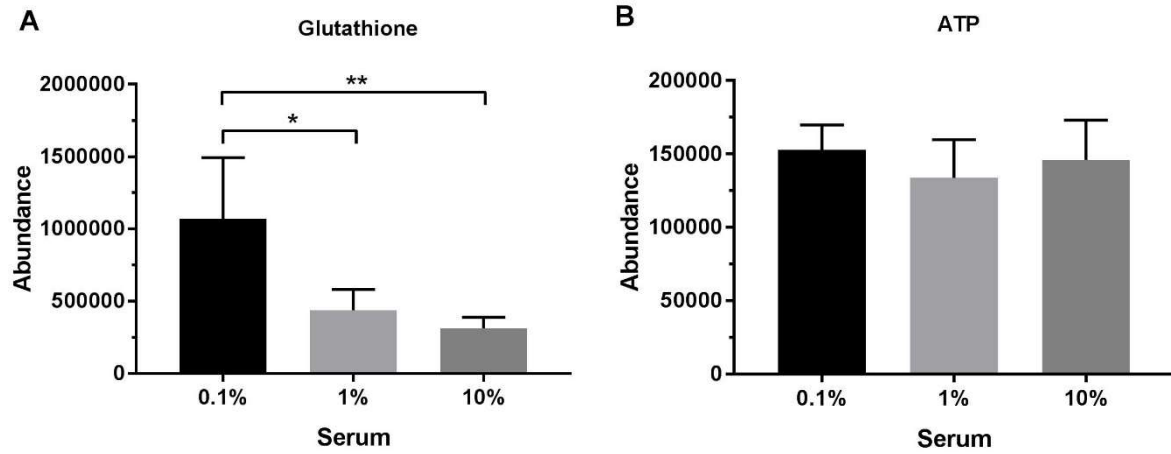


Figure 24 - The abundance of glutathione and ATP in 10%, 1% and 0.1% FBS cultures. (A) Glutathione abundance decreases when higher levels of serum are present. (B) ATP levels appear consistent across the three conditions and there are no significant differences.

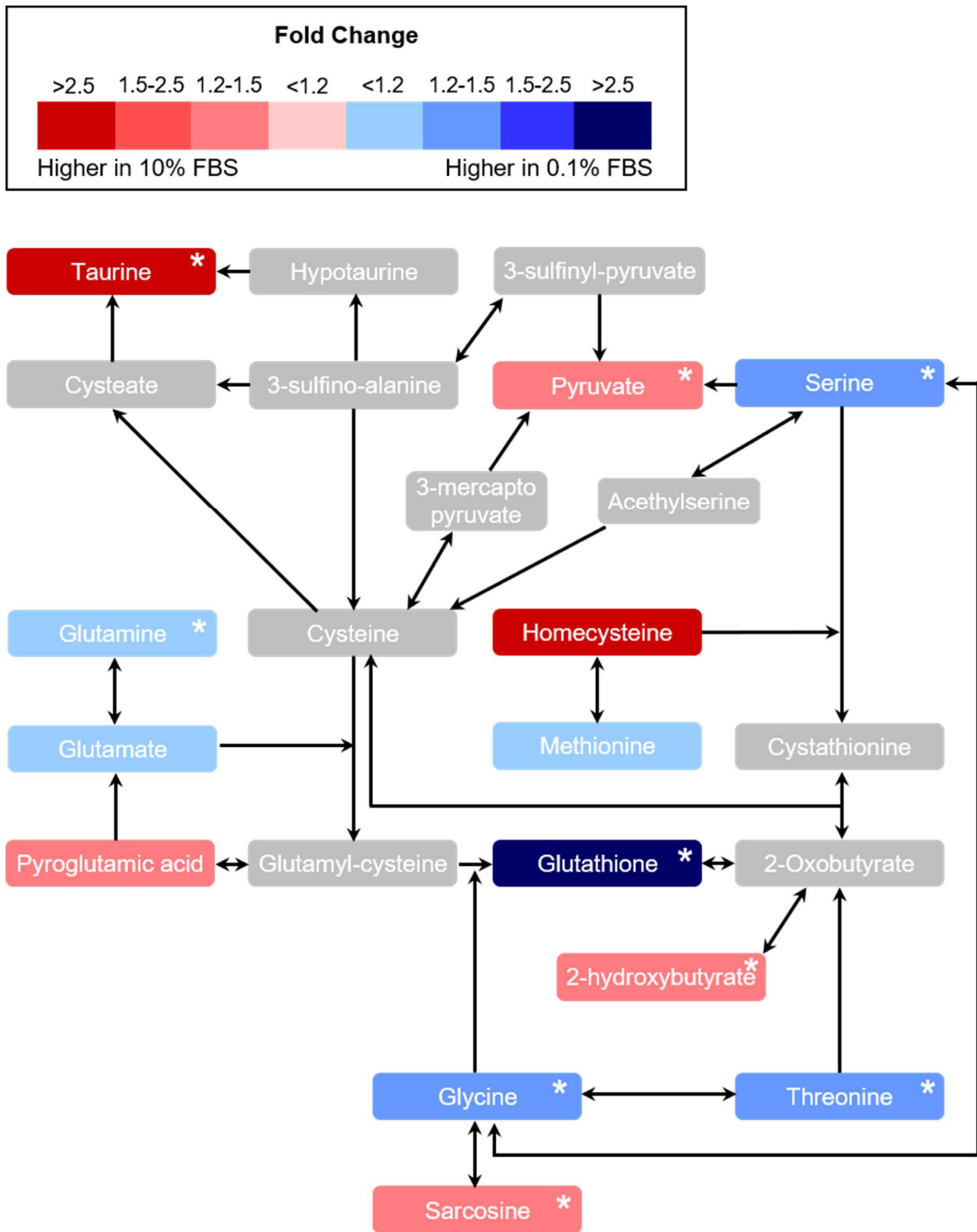


Figure 25 - Amino acid catabolism pathways surrounding glutathione: fold changes in 10% vs 0.1% FBS cultures. The fold change is indicated by the colour of the boxes and all significant changes are denoted with a single asterisk. Note that the fold change of homocysteine is 'infinity' as it was not detected in the 0.1% FBS samples. Compounds in grey boxes were not identified.

4. Discussion

The experiments presented here show that the culture environment in which cells are grown can impact their metabolism. This means that care must be taken to use appropriate conditions in *in vitro* studies to ensure that effects on the parameter being measured are not being improperly influenced by the culture conditions.

4.1 Glucose

Initially, glucose was shown to suppress oxygen consumption (see Figure 6). This phenomenon has been previously reported [31, 32] and the data here suggest that CHO cells are susceptible to the Crabtree effect. Oxygen consumption in cells cultured in high glucose may be suppressed by a number of mechanisms. Firstly, the presence of higher ATP levels along with the high glucose concentration itself [12] mean AMPK is likely inactive in these cells. AMPK activation has been shown to increase mitochondrial biogenesis and β -oxidation of fatty acids [12, 13], so maintaining AMPK in its inactive form will prevent stimulation of these processes which would otherwise encourage oxygen consumption. The converse is also true; the slightly decreased ATP level in glucose free cultures could trigger AMPK activation and thus an increase in OXPHOS. Additionally, F16BP has been shown to attenuate ETC activity [36]. In high glucose cultures, higher glycolytic flux will result in greater accumulation of this intermediate within cells, offering another explanation for the reduction in OXPHOS seen. Inhibition of ChREBP activity through siRNA treatment was shown to increase oxygen consumption [30]. Since ChREBP is active when glucose is readily available, OXPHOS is not stimulated. On the other hand, cells cultured in low glucose would not activate ChREBP, stimulating oxygen consumption.

These signalling pathways could explain why the Crabtree effect is seen in these cells, but further investigation is needed to confirm whether they are indeed active. For example, ChREBP is active when localised to the nucleus as it functions as a transcription factor. When glucose is present in excess, ChREBP is dephosphorylated and can enter the nucleus. Immunofluorescent microscopy using a ChREBP specific antibody could confirm both expression of the protein by CHO cells and its subcellular localisation. Furthermore, activity of AMPK could be assessed using a Western blot if antibodies specific to T172-phosphorylated AMPK are used.

The cells cultured in 10mM glucose are able to meet their energetic requirements despite a decrease in OXPHOS, as shown by consistent growth and ATP levels (see Figure 6). Since the yield of ATP per glucose molecule is significantly reduced in glycolysis compared to OXPHOS, this suggests an increase in glycolytic flux is required to meet ATP demands. This could be tested by measuring the extracellular acidification rate of the culture medium under various glucose concentrations, as acidification is indicative of glycolytic flux due to the production of lactic acid. Research by Potter et al. [31] has shown that cells under high glucose do indeed appear to upregulate glycolysis.

4.2 Glutamine

Under glucose limiting conditions, cells switch to using their mitochondria and producing ATP through the TCA cycle and OXPHOS, demonstrating that CHO cells have metabolic flexibility and can adapt their metabolism to substrate availability accordingly. For oxygen consumption to increase, there must be a suitable substrate(s) available to drive the production of reducing equivalents. In many cultures, this substrate is glutamine. As shown in Figure 8, glutamine is required for

the increase in OCR seen when glucose is limiting in CHO cells. This supports the idea that, in these cells, glutamine is feeding into the TCA cycle via glutamate. To confirm whether this is the case, catabolism of glutamine by glutaminase could be inhibited using siRNA and the OCR again measured.

4.3 Lactate

When lactate is added to the culture media, ATP levels remain stable and cell number is consistent. This shows that up to 10mM lactate is not detrimental to CHO cell health. However, it is interesting to note the reduction in cell number when glutamine is removed from these cultures. This is suggestive of glutamine being used as an energy source which is also reflected in the OCR.

Lactate, on the other hand, does not appear to be used as an energy source. It had no effect on cell number or ATP, and the OCR data are inconclusive (see Figures 9 and 10). It would be expected that, if CHO cells were taking up and metabolising lactate, the OCR would increase. This is because lactate would be converted into pyruvate via LDH and thus feed into the TCA cycle. As lactate is an end product of glycolysis, it cannot produce ATP through the glycolytic pathway. There is a lot of research surrounding CHO cells and their ability to consume lactate, particularly in the biopharmaceutical industry. CHO cells in bioreactors can consume lactate that accumulates in their culture environment [44, 78, 79]. However, the results presented here show little evidence of this. It is possible that the lactate in these cultures was not taken up by the CHO cells. Lactate enters cells through a monocarboxylate transporter, which co-transporters lactate and H^+ . The direction of this transporter is driven by the relative concentration of lactate and H^+ across the plasma membrane [80]. Because sodium lactate was supplemented, rather than lactic acid, it is possible that cells were unable to absorb the lactate in the culture

medium effectively. This has been demonstrated in HEK293 cells, whereby sodium lactate could not trigger lactate consumption but lactic acid could [81].

In the first experiment (see Figure 9), lactate appeared to suppress oxygen consumption. This has interesting implications as the effect is similar to that displayed when cells are cultured in excess glucose. Under these conditions, cells are likely relying on glycolysis to meet their ATP requirements, which means that lactate will be produced. This means the lactate concentration in the culture medium increases. It is possible that the effect excess glucose has on the OCR could, in part, be conferred by the lactate it produces rather than the glucose itself. However, because the effect of lactate on OCR was not observed when the experiment was repeated (see Figure 10), further investigations are required to confirm which is the true effect.

In the lactate experiments, cells were deprived of glucose. This means that under the 0mM lactate and 0mM glutamine conditions, cells were deprived of glucose, glutamine, pyruvate and lactate. Thus, amino acids (glycine, arginine, cysteine, histidine, isoleucine, leucine, lysine, methionine, phenylalanine, proline, serine, threonine, tryptophan, tyrosine and valine) were the only fuel source provided by the culture medium, but cells were still able to maintain their ATP levels. As the assay used here measures steady state ATP levels, this is not reflective of ATP turnover. Given that these cells also exhibited decreased growth, it is likely that these cells were not producing ATP at the same rate, but had compensated for this by curbing ATP consuming processes. This would mean a greater proportion of cells were quiescent and would explain the decrease in cell growth. If the incubation period in this medium were extended, ATP levels would be expected to fall.

4.4 FBS

Reducing the serum concentration impacted on cell growth. This was expected since serum contains high levels of growth factors. The increase in cell death may also be explained by this, as reducing the serum concentration results in a reduction in survival factors present in the media. However, reducing the serum content also increases the sensitivity of the cells to shear stress and trypsinisation. Trypsin is inhibited by α 1-antitrypsin which is found in serum [47] while albumin has been shown to protect cells against shear stress [82]. This means that cells detach from the culture surface more quickly and suffer more stress during the passage process. Because of this, the increase in percentage cell death demonstrated in Figure 14 could be a by-product of the passaging and seeding process required to set up the plates, rather than a direct effect of serum deprivation.

The elongation of cells grown in reduced serum has also been observed in fibroblasts (Dombi 2017, unpublished data). Although there is no clear explanation as to why this may occur, it may be that this is a result of the decrease in growth rate which occurs when cells are exposed to a low serum environment. In 10% FBS, the growth rate is high which means the time between mitoses is smaller. This allows less time for each individual cell to flatten and adhere to the culture surface between cell division events, possibly explaining the change in cell shape seen in Figure 13. Another explanation is that the change in availability of growth factors and hormones drives alterations in gene expression patterns which affect the cell phenotype.

Interpretation of the metabolomics data lead to several key observations. Firstly, there appear to be changes in metabolites involved in the response to oxidative stress. Reduced glutathione (GSH) is decreased in cells cultured in 10% FBS (see

Figure 24), and there are alterations in the pathways surrounding glutathione synthesis (see Figure 25). The decrease in GSH could be a result of a decrease in total glutathione availability, or specifically in the availability of the reduced form. From this data alone, two conclusions could be drawn. The first is that cells cultured in 0.1% FBS are experiencing more oxidative stress and have upregulated glutathione synthesis to compensate, increasing the total glutathione pool. The other explanation is that cells cultured in 10% FBS are experiencing more oxidative stress, meaning the GSH pool is decreased with a concomitant increase in oxidised glutathione (GSSG). Because GSSG was not an identified metabolite, which cells are under more oxidative stress cannot be easily determined.

However, several other factors suggest that cells cultured in 10% FBS experience more oxidative stress. Firstly, homocysteine was detected in 10% FBS cultured cells but not in either of the low serum conditions. Homocysteine is an intermediate in the methionine degradation pathway which produces cysteine. Typically, a lack of cysteine is the rate limiting step in glutathione synthesis [83], therefore the presence of this metabolite suggests that cells are attempting to replenish cysteine levels which may have dropped. This is further supported by the increase in 2-hydroxybutyrate seen in 10% FBS cultures, as this is also a by-product of cysteine production from methionine. Glutamate-cysteine ligase is the rate limiting enzyme in glutathione synthesis and is under tight regulation [83]. Its activity can be upregulated in response to oxidative stress [83]. This shows that if cells in the 10% FBS condition were indeed experiencing more oxidative stress, then they have the potential to upregulate glutathione synthesis in response to this.

Additionally, glycine, another component of glutathione, was significantly lower in 10% FBS cultures when compared to 0.1% FBS cultures (see Figure 25). This

points to a higher usage of glycine, potentially due to increased glutathione production. Furthermore, sarcosine is increased in 10% FBS cultures. This amino acid is an intermediate in glycine synthesis, so its increased abundance indicates glycine synthesis is being upregulated despite the glycine concentration being reduced. Carnosine, a dipeptide molecule comprised of alanine and histidine, is also exclusively found in 10% FBS cultures and is a known antioxidant [84]. Since the production of carnosine by carnosine synthase is an ATP dependent process [85], the synthesis of this compound is likely under tight control. It can therefore be assumed that its production only occurs when necessary and that the 10% FBS containing cultures must be experiencing oxidative stress. The presence of pyroglutamic acid at higher levels in the 10% FBS condition also points to increased oxidative stress as pyroglutamic acid is an intermediate in glutathione degradation. This would imply a greater turnover of glutathione.

The regeneration of GSH from GSSG by glutathione reductase requires the reducing power of NADPH. NADPH production in the cell occurs primarily in the pentose phosphate pathway. Unfortunately, no components of this pathway were identified in the metabolomics data set so no indication of the flux through this pathway can be inferred. However, two other key NADPH producing reactions exist. These are reactions catalysed by the NADP-dependent malic enzyme (malate + $\text{NADP}^+ \leftrightarrow$ pyruvate + CO_2 + NADPH) and glutamate dehydrogenase (glutamate + H_2O + $\text{NADP}^+ \leftrightarrow$ α -ketoglutarate + NH_3 + NADPH + H^+). In both cases, the concentrations of the products were higher while the concentrations of the reactants were lower in cells cultured in 10% FBS (see Figure 22). This indicates that these cells are inclined towards NADPH producing reactions, potentially which the aim of regenerating GSH from GSSG.

The enzyme glutathione peroxidase is an important antioxidant enzyme. It catalyses the oxidation of GSH and concomitant reduction of hydrogen peroxide into water [86]. Incidentally, glutathione peroxidase is a selenium containing enzyme [86]. Because FBS contains selenium, but the base medium does not, the activity of this enzyme in serum containing cultures is likely higher. This could also explain the decrease in GSH. Glutathione peroxidase activity will increase due to the presence of its cofactor, meaning more glutathione will be oxidised by the enzyme.

Since OXPHOS was increased in the 10% FBS containing culture, this could offer an explanation as to the need for more glutathione. An increase in electron transport does not cause an increase in ROS *per se*. However, an increase in substrates which feed into the ETC causes an increase in the reduction state of the ETC and thus increases the rate of ROS production. In this case, the increase in TCA cycle intermediates seen in cells cultured in 10% FBS could be a causative factor in the increase in ROS which would accompany the decrease in GSH abundance [74]. In particular, FADH₂ has been shown to reduce molecular oxygen. The increased abundance of succinate in 10% FBS cultures would cause an increase in FADH₂ production by succinate dehydrogenase. Additionally, succinate dehydrogenase contains iron-sulphur clusters. The presence of iron and transferrin in serum could thereby cause an upregulation in the activity of this enzyme, producing FADH₂ at a greater rate and causing more ROS to be generated [87]. Commercially available kits which measure the GSH:GSSG ratio could be used to confirm which cultures are under greater levels of oxidative stress.

The accumulation of the polyol sorbitol in 10% FBS cultures is indicative of excess glucose and could be the reason for the increase in oxidative stress observed in these cells. In the body, when hyperglycaemia occurs, glucose saturates the

hexokinase enzyme [88]. Glucose is then diverted into the polyol pathway, and sorbitol is formed from glucose through the action of aldose reductase [89]. This reaction uses NADPH as a cofactor and generates NADP⁺. Thus, the increase in sorbitol seen in 10% FBS cultures will likely be accompanied by a decrease in the NADPH:NADP⁺ ratio. This could account for the decrease in GSH observed in these cells, as cells cannot effectively regenerate GSH from GSSG. Cells in all serum concentrations were cultured under the same glucose concentration (7mM). Because of this, one would expect to see similar levels of sorbitol accumulation in all experimental conditions. However, this was not the case. The presence of insulin in serum could be used to explain these differences. Although the cells in reduced serum cultures are maintained under relatively high glucose concentrations, the lack of insulin means that glucose may not enter these cells rapidly enough to saturate glycolytic capacity. On the other hand, cells cultured in 10% FBS are exposed to insulin and the transport of glucose into these cells is likely higher. This means that glucose can accumulate inside the cells to the point where it saturates the hexokinase enzyme and sorbitol is produced.

Taurine levels increased significantly with increasing serum concentration, showing the largest fold difference out of any identified metabolite. Taurine is found at micromolar levels [90] in human plasma, so it is possible that the striking increase in taurine is caused not by a change in metabolism, but simply because taurine is added to cells as a component of the serum. On the other hand, taurine is synthesised from cysteine. If the cells cultured in 10% FBS are indeed producing taurine at a higher rate, this could offer an alternative explanation for the changes surrounding cysteine metabolism observed (see Figure 25). The argument for increased taurine production is supported by the enzyme hypotaurine

dehydrogenase and its requirement for a haem cofactor [91]. Hypotaurine dehydrogenase catalyses the production of taurine from hypotaurine. The presence of iron and transferrin in serum may then have allowed this reaction to proceed at a greater rate, explaining the higher abundance of taurine in higher serum cultures.

Interestingly, all non-essential (excluding conditionally essential) amino acids were found at higher concentrations in the 0.1% FBS cultures. Since all proteinogenic amino acids are provided by the culture medium, the reason for this change is unclear. Glutamine, glutamate, asparagine and aspartate can all feed into the TCA cycle in anaplerotic reactions. The accumulation of these amino acids, particularly asparagine, in 0.1% FBS cultures could be indicative of reduced total flux through the TCA cycle, hence less need for amino acid catabolism to replenish intermediates. There is an increase in urea in 10% FBS cultures which could indicate increased breakdown of amino acids in reactions such as these. This is further supported by the presence of ornithine in 10% FBS cultures, as this is a component in the urea cycle and is suggestive of increased amino acid catabolism. The triiodothyronine hormone which is present in serum also upregulates mitochondrial oxidative capabilities, again explaining the need for more anaplerosis. [66]. The increase in OCR measured in cells cultured in 10% FBS also supports this conclusion.

2-hydroxyglutarate is formed from the TCA cycle intermediate α -ketoglutarate. It is accumulated in 0.1% FBS cultures when compared to 10% FBS cultures. This metabolite has been shown to inhibit α -ketoglutarate dependent histone demethylases [92]. This shows how altering the metabolic profile of the cell through culture conditions has the potential to exert widespread effects on the cell. In this instance, this metabolite affects epigenetic regulation of the gene expression.

Glycerol 3-phosphate is significantly higher in the 0.1% FBS cultures than in the other two conditions. This metabolite is part of a redox balancing reaction where the conversion of glycerol 3-phosphate and dihydroxyacetone phosphate (DHAP) is catalysed by glycerol 3-phosphate dehydrogenase 1. Although DHAP was not identified in these experiments, glycerol 3-phosphate being more abundant in the 0.1% FBS condition while glycerol levels remained comparable is suggestive of redox balancing. 0.1% FBS cells have a lower OCR (see Figure 14), implying they are not conducting efficient OXPHOS. This would mean other ATP producing reactions, such as those found in glycolysis, would have to be upregulated to meet the energy demands of the cell. The conversion of DHAP to glycerol 3-phosphate produces NAD^+ , which is a required cofactor in glycolysis. However, the theory that glycolytic flux is upregulated in low serum cultures is not supported by the pyruvate/lactate ratio which is marginally increased in 0.1% FBS cells compared the other conditions (0.1% = 0.365, 1% = 0.356, 10% = 0.308). However, this does not account for the excretion of lactate through the monocarboxylate transporter, which is known to occur in CHO cells [93]. Glycerol 3-phosphate also acts as a shuttle which transfers reducing power from the cytosol to the mitochondrial ETC. The conversion of glycerol 3-phosphate to DHAP can be catalysed at the inner mitochondrial membrane by glycerol 3-phosphate dehydrogenase 2. This reaction reduces FAD to FADH_2 which feeds electrons directly into the ETC. Since a build-up of glycerol 3-phosphate occurs while the OCR is significantly reduced in 0.1% FBS cells, it is possible that this reaction is slowed under reduced serum conditions. This could be due to impairment of the ETC, potentially caused by a lack of iron transport into cells due to transferrin deprivation.

Experiments using the luminescent ATP kit showed a decrease in ATP in cells cultured in 10% FBS (see Figure 14). This effect was not shown in the metabolomics data, with similar ATP values being found across all three conditions (see Figure 24). This discrepancy could be explained in a number of ways. Firstly, because standard curves were not constructed when measuring ATP using luminescence, the concentration of ATP is unknown. This means that ATP levels may be low, so although there are significant changes in the ATP levels in these samples, the actual changes may be very small. In this case, small absolute changes in the ATP may not be detected using mass spectrometry.

Interestingly, the lowest serum concentration tested resulted in a slight increase in creatinine. Creatinine functions as a store of chemical energy which is able to quickly replenish ATP [94]. An increase in creatinine suggests that cells cultured in low serum may be better able to replenish ATP if the concentration does drop. This could also be the cause of the conflicting ATP results obtained. In the plate based assay, ATP hydrolysis is quenched using an inhibitor(s) to maintain cellular ATP levels. However, this effect will not be instantaneous. It is possible that during this window, the 0.1% FBS cells were able to replenish some of their ATP using phosphocreatine before the degradation reactions were fully quenched, thus resulting in higher ATP levels being recorded. The robustness of normalisation methods could also be a factor. Both samples were normalised to DNA content, but measurements for DNA were obtained using either a fluorescent stain (PI) or by extraction and quantification by absorbance at 260nm wavelength.

The metabolomics data, along with the increase in oxygen consumption seen in 10% FBS cells, suggests an increase in fatty acid β -oxidation in these cells. Firstly, there is a slight increase in glycerol, indicative of triglyceride lipolysis. Secondly,

citrate and its isomer mesoconic acid, are increased in 10% FBS cultures. The acetyl CoA formed from β -oxidation of fatty acids condenses with oxaloacetate to enter the TCA cycle, forming citrate. An increase in N,N,N-trimethyllysine is seen in 10% FBS cultures. This metabolite is required for the production of carnitine, which shuttles long-chain fatty acids across the inner mitochondrial membrane for oxidation [95]. This means the increase in N,N,N-trimethyllysine could reflect increased β -oxidation in cells cultured in high serum. Fatty acids are found in FBS, typically bound to albumin. This increased presence of fatty acids in cultures with a higher percentage of FBS would explain the apparent increase in β -oxidation.

However, the increase in citrate seen in 10% FBS cultures could also be reflective of increased fatty acid synthesis. Citrate is exported from the mitochondria where it is broken down into acetyl CoA and oxaloacetate. Acetyl CoA is then used to synthesise fatty acids in the cytoplasm. In this sense, citrate is used to shuttle acetyl CoA from the mitochondria to the cytoplasm. When cells divide, new cell and organelle membranes must be produced, all containing fatty acids, predominantly in the form of phospholipids. An increase in fatty acid synthesis would therefore be expected in cells cultured in 10% FBS due to their increased rate of proliferation.

The early stages of glycolysis appear to be increased in low serum cultures, with glucose 6-phosphate and F16BP both being more abundant. Interestingly, these are both metabolites formed by rate controlling reactions in glycolysis. Pyruvate, on the other hand, was increased in 10% serum cultures and is also the product of a rate controlling reaction which is catalysed by pyruvate kinase. Why the levels of these glycolytic intermediates change in different directions cannot be easily explained. The pentose phosphate pathway runs parallel to glycolysis, and could shed some light upon the fate of the glycolytic intermediates. However, no pentose

phosphate pathway metabolites were detected in this study. It is possible that, since cell growth was increased in 10% FBS cultures, more glycolytic intermediates were diverted to the pentose phosphate pathway to meet the demand for nucleotides required for DNA synthesis. This would explain the decrease in glucose 6-phosphate. Lactate concentrations were also higher in 10% FBS cultures, indicating higher glycolytic flux.

Enzymes surrounding the synthesis and degradation of glycogen are upregulated in 0.1% FBS cultures. Glucose 1-phosphate is an intermediate in both glycogen synthesis and glycogenolysis, so this alone could not indicate which direction the reaction was proceeding in. Uridine diphosphate-glucose (UDP-glucose) however, is produced only in the glycogenesis reaction. It is produced from glucose 6-phosphate, via glucose 1-phosphate (see Figure 22) and is subsequently added to a growing polysaccharide chain. Thus, the presence of this metabolite suggests glycogen is being synthesised in serum starved cells. This is counterintuitive, as the presence of insulin in serum would be expected to stimulate glycogen synthesis [96], meaning one would expect to see an increase in glycogen synthesis in cells cultured in higher serum conditions. However, glycogen synthase is allosterically activated by glucose 6-phosphate [96], which was more abundant in the 0.1% FBS condition. In fact, glucose 6-phosphate was shown to have a greater influence on glycogen synthase activity than insulin [97]. This could explain the increase in glycogen synthesis which is apparently observed. As the data on ATP concentration was not consistent across the two methods used, it is difficult to reconcile. However, if it was found that ATP levels were indeed elevated in the low serum cultures, this could explain increased glycogen storage. ATP is an inhibitor of the glycogen phosphorylase enzyme which hydrolyses glycogen, meaning a decrease in

glycogen breakdown would occur [98]. Glycogen can be visualised using methods such as Periodic acid–Schiff staining [99]. This could confirm whether there was indeed a greater amount of glycogen present in cells cultured in a reduced serum environment.

5. Concluding Remarks

The data presented in this project show how the components of cell culture media can have a drastic impact on cell metabolism. The availability of carbon substrates impacts on OXPHOS, with high concentrations of glucose inhibiting OXPHOS, while glutamine supports oxygen consumption when cells are deprived of glucose. Serum, an almost ubiquitous cell culture supplement, also had a significant impact on metabolism. Cells cultured in 10% FBS showed a more oxidative phenotype, with apparent increases in oxidative stress and TCA cycle activity. As FBS is an undefined factor, its impact on metabolism is largely unaccounted for and batch to batch variation has the potential to impact experimental results.

Future directions should include more in-depth analysis of the pathways involved in these adaptation systems. For example, the mechanisms by which cells switch between glycolytic and oxidative phenotypes could be elucidated using techniques to measure expression of key metabolic-state sensing enzymes and their downstream effectors. siRNA or chemical inhibitors could be used to manipulate these pathways.

With regards to serum, testing the impact of different batches of serum from suppliers across different continents on cell metabolism would be beneficial. The data here have shown that the concentration of serum added to cell culture media impacts the cellular phenotype. It would be interesting to investigate whether batch to batch variation can cause such drastic effects. Since the use of serum is so widespread, this is relevant across the scientific community and could account for much of the variation observed in *in vitro* systems.

Acknowledgements

I would like to thank my supervisor Dr. Karl Morten for his direction and support during the course of this project, and for answering my never-ending questions. I would also like to express my gratitude to Dr. Tracy Walker and Vicky Chung at GlaxoSmithKline for their guidance and excellent proof-reading skills! I also acknowledge the contribution of my second supervisor Prof. James McCullagh and his team at the Chemistry Research Lab for processing and analysing the metabolomics samples.

References

1. Luxcel Biosciences. *MitoXpress Xtra Oxygen Consumption Assay User Manual*. 2017 [cited 2017 17 August]; Available from: <http://luxcel.com/content/mitoxpress-xtra-oxygen-consumption-assay-user-manual>.
2. Berg, J.M., J.L. Tymoczko, and L. Stryer, *The Glycolytic Pathway Is Tightly Controlled*. 2002.
3. Li, X.B., J.D. Gu, and Q.H. Zhou, *Review of aerobic glycolysis and its key enzymes - new targets for lung cancer therapy*. Thoracic Cancer, 2015. **6**(1): p. 17-24.
4. Wilcox, G., *Insulin and Insulin Resistance*, in *Clin Biochem Rev*. 2005. p. 19-39.
5. Vegiopoulos, A. and S. Herzig, *Glucocorticoids, metabolism and metabolic diseases*. Molecular and Cellular Endocrinology, 2007. **275**(1-2): p. 43-61.
6. Berg, J.M., J.L. Tymoczko, and L. Stryer, *Cells Can Respond to Changes in Their Environments*. 2002, W H Freeman.
7. Lewis, M., *The lac repressor*. Comptes Rendus Biologies, 2005. **328**(6): p. 521-548.
8. Fridlyand, L.E. and L.H. Philipson, *Glucose sensing in the pancreatic beta cell: a computational systems analysis*. Theoretical Biology and Medical Modelling, 2010. **7**: p. 44.
9. Fu, Z., E.R. Gilbert, and D. Liu, *Regulation of insulin synthesis and secretion and pancreatic Beta-cell dysfunction in diabetes*. Curr Diabetes Rev, 2013. **9**(1): p. 25-53.
10. Kawaguchi, T., et al., *Glucose and cAMP regulate the L-type pyruvate kinase gene by phosphorylation/dephosphorylation of the carbohydrate response element binding protein*. Proceedings of the National Academy of Sciences of the United States of America, 2001. **98**(24): p. 13710-13715.
11. Tokunaga, C., K. Yoshino, and K. Yonezawa, *mTOR integrates amino acid- and energy-sensing pathways*. Biochemical and Biophysical Research Communications, 2004. **313**(2): p. 443-446.
12. Jeon, S.M., *Regulation and function of AMPK in physiology and diseases*. Experimental and Molecular Medicine, 2016. **48**: p. 13.
13. Lin, J.D., C. Handschin, and B.M. Spiegelman, *Metabolic control through the PGC-1 family of transcription coactivators*. Cell Metabolism, 2005. **1**(6): p. 361-370.
14. Saxton, R.A. and D.M. Sabatini, *mTOR Signaling in Growth, Metabolism, and Disease*. Cell, 2017. **168**(6): p. 960-976.
15. Wullschlegel, S., R. Loewith, and M.N. Hall, *TOR signaling in growth and metabolism*. Cell, 2006. **124**(3): p. 471-484.
16. Choo, A.Y., et al., *Rapamycin differentially inhibits S6Ks and 4E-BP1 to mediate cell-type-specific repression of mRNA translation*. Proceedings of the National Academy of Sciences of the United States of America, 2008. **105**(45): p. 17414-17419.
17. Scherer, W.F., J.T. Syverton, and G.O. Gey, *STUDIES ON THE PROPAGATION IN VITRO OF POLIOMYELITIS VIRUSES : IV. VIRAL MULTIPLICATION IN A STABLE STRAIN OF HUMAN MALIGNANT EPITHELIAL CELLS (STRAIN HELA) DERIVED FROM AN EPIDERMOID CARCINOMA OF THE CERVIX*. J Exp Med, 1953. **97**(5): p. 695-710.
18. Crabtree, H.G., *Observations on the carbohydrate metabolism of tumours*. Biochem J, 1929. **23**(3): p. 536-45.
19. Heiskanen, A., J. Emneus, and M. Dufva, *PERFUSION BASED CELL CULTURE CHIPS*. Microfluidics Based Microsystems: Fundamentals and Applications, 2010: p. 427-452.

20. Hirt, C., et al., *Bioreactor-engineered cancer tissue-like structures mimic phenotypes, gene expression profiles and drug resistance patterns observed "in vivo"*. *Biomaterials*, 2015. **62**: p. 138-146.
21. Toh, Y.C., et al., *A novel 3D mammalian cell perfusion-culture system in microfluidic channels*. *Lab on a Chip*, 2007. **7**(3): p. 302-309.
22. Habler, O.P. and K.F.W. Messmer, *The physiology of oxygen transport*. *Transfusion Science*, 1997. **18**(3): p. 425-435.
23. Suckale, J. and M. Solimena, *Pancreas islets in metabolic signaling - focus on the beta-cell*. *Frontiers in Bioscience-Landmark*, 2008. **13**: p. 7156-7171.
24. Inoguchi, T., et al., *High glucose level and free fatty acid stimulate reactive oxygen species production through protein kinase C-dependent activation of NAD(P)H oxidase in cultured vascular cells*. *Diabetes*, 2000. **49**(11): p. 1939-1945.
25. Quagliaro, L., et al., *Intermittent high glucose enhances apoptosis related to oxidative stress in human umbilical vein endothelial cells. The role of protein kinase C and NAD (P) H oxidase activation*. *Diabetes*, 2003. **52**: p. A178-A178.
26. Yu, T.Z., et al., *Mitochondrial fission mediates high glucose-induced cell death through elevated production of reactive oxygen species*. *Cardiovascular Research*, 2008. **79**(2): p. 341-351.
27. El-Osta, A., et al., *Transient high glucose causes persistent epigenetic changes and altered gene expression during subsequent normoglycemia*. *Journal of Experimental Medicine*, 2008. **205**(10): p. 2409-2417.
28. Uyeda, K. and J.J. Repa, *Carbohydrate response element binding protein, ChREBP, a transcription factor coupling hepatic glucose utilization and lipid synthesis*. *Cell Metabolism*, 2006. **4**(2): p. 107-110.
29. Yu, Y.J., T.G. Maguire, and J.C. Alwine, *ChREBP, a glucose-responsive transcriptional factor, enhances glucose metabolism to support biosynthesis in human cytomegalovirus-infected cells*. *Proceedings of the National Academy of Sciences of the United States of America*, 2014. **111**(5): p. 1951-1956.
30. Tong, X.M., et al., *The glucose-responsive transcription factor ChREBP contributes to glucose-dependent anabolic synthesis and cell proliferation*. *Proceedings of the National Academy of Sciences of the United States of America*, 2009. **106**(51): p. 21660-21665.
31. Potter, M., E. Newport, and K.J. Morten, *The Warburg effect: 80 years on*. *Biochemical Society Transactions*, 2016. **44**: p. 1499-1505.
32. Marroquin, L.D., et al., *Circumventing the crabtree effect: Replacing media glucose with galactose increases susceptibility of HepG2 cells to mitochondrial toxicants*. *Toxicological Sciences*, 2007. **97**(2): p. 539-547.
33. Rossignol, R., et al., *Energy substrate modulates mitochondrial structure and oxidative capacity in cancer cells*. *Cancer Research*, 2004. **64**(3): p. 985-993.
34. Diaz-Ruiz, R., et al., *Tumor cell energy metabolism and its common features with yeast metabolism*. *Biochimica Et Biophysica Acta-Reviews on Cancer*, 2009. **1796**(2): p. 252-265.
35. Diaz-Ruiz, R., M. Rigoulet, and A. Devin, *The Warburg and Crabtree effects: On the origin of cancer cell energy metabolism and of yeast glucose repression*. *Biochimica Et Biophysica Acta-Bioenergetics*, 2011. **1807**(6): p. 568-576.
36. Diaz-Ruiz, R., et al., *Mitochondrial oxidative phosphorylation is regulated by fructose 1,6-bisphosphate - A possible role in Crabtree effect induction?* *Journal of Biological Chemistry*, 2008. **283**(40): p. 26948-26955.
37. Brosnan, J.T., *Interorgan amino acid transport and its regulation*. *Journal of Nutrition*, 2003. **133**(6): p. 2068S-2072S.
38. Curi, R., et al., *Glutamine, gene expression, and cell function*. *Frontiers in Bioscience*, 2007. **12**: p. 344-357.
39. Medline Plus. *Plasma amino acids*. 2015 [cited 2017 10 August].
40. Shimmura, C., et al., *Alteration of Plasma Glutamate and Glutamine Levels in Children with High-Functioning Autism*. *Plos One*, 2011. **6**(10): p. 6.

41. Jin, L., G.N. Alesi, and S. Kang, *Glutaminolysis as a target for cancer therapy*. *Oncogene*, 2016. **35**(28): p. 3619-3625.
42. Lavoigne, A., et al., *Glutamine inhibits the lowering effect of glucose on the level of phosphoenolpyruvate carboxykinase mRNA in isolated rat hepatocytes*. *European Journal of Biochemistry*, 1996. **242**(3): p. 537-543.
43. Luo, J., et al., *Comparative metabolite analysis to understand lactate metabolism shift in Chinese hamster ovary cell culture process*. *Biotechnology and Bioengineering*, 2012. **109**(1): p. 146-156.
44. Zagari, F., et al., *Lactate metabolism shift in CHO cell culture: the role of mitochondrial oxidative activity*. *New Biotechnology*, 2013. **30**(2): p. 238-245.
45. Gladden, L.B., *Lactate metabolism: a new paradigm for the third millennium*. *Journal of Physiology-London*, 2004. **558**(1): p. 5-30.
46. Leite, T.C., et al., *Lactate favours the dissociation of skeletal muscle 6-phosphofructo-1-kinase tetramers down-regulating the enzyme and muscle glycolysis*. *Biochemical Journal*, 2007. **408**: p. 123-130.
47. van der Valk, J., et al., *Optimization of chemically defined cell culture media - Replacing fetal bovine serum in mammalian in vitro methods*. *Toxicology in Vitro*, 2010. **24**(4): p. 1053-1063.
48. Pazos, P., et al., *Culturing cells without serum: Lessons learnt using molecules of plant origin*. *Altex-Alternativen Zu Tierexperimenten*, 2004. **21**(2): p. 67-72.
49. van der Valk, J., et al., *The humane collection of fetal bovine serum and possibilities for serum-free cell and tissue culture*. *Toxicology in Vitro*, 2004. **18**(1): p. 1-12.
50. Gstraunthaler, G., *Alternatives to the use of fetal bovine serum: Serum-free cell culture*. *Altex-Alternativen Zu Tierexperimenten*, 2003. **20**(4): p. 275-281.
51. Iwase, H., et al., *The ratio of insulin to C-peptide can be used to make a forensic diagnosis of exogenous insulin overdose*. *Forensic Science International*, 2001. **115**(1-2): p. 123-127.
52. Dimitriadis, G., et al., *Insulin effects in muscle and adipose tissue*. *Diabetes Research and Clinical Practice*, 2011. **93**: p. S52-S59.
53. Strohl, W.R., *Fusion Proteins for Half-Life Extension of Biologics as a Strategy to Make Biobetters*. *Biodrugs*, 2015. **29**(4): p. 215-239.
54. Tortorella, S. and T.C. Karagiannis, *Transferrin Receptor-Mediated Endocytosis: A Useful Target for Cancer Therapy*. *Journal of Membrane Biology*, 2014. **247**(4): p. 291-307.
55. Chung, M.C.M., *STRUCTURE AND FUNCTION OF TRANSFERRIN*. *Biochemical Education*, 1984. **12**(4): p. 146-154.
56. Xu, W.J., T. Barrientos, and N.C. Andrews, *Iron and Copper in Mitochondrial Diseases*. *Cell Metabolism*, 2013. **17**(3): p. 319-328.
57. Walter, P.B., et al., *Iron deficiency and iron excess damage mitochondria and mitochondrial DNA in rats*. *Proceedings of the National Academy of Sciences of the United States of America*, 2002. **99**(4): p. 2264-2269.
58. Bresgen, N. and P.M. Eckl, *Oxidative Stress and the Homeodynamics of Iron Metabolism*. *Biomolecules*, 2015. **5**(2): p. 808-847.
59. Arigony, A.L.V., et al., *The Influence of Micronutrients in Cell Culture: A Reflection on Viability and Genomic Stability*. *Biomed Research International*, 2013: p. 22.
60. Helmy, M.H., et al., *Effect of selenium supplementation on the activities of glutathione metabolizing enzymes in human hepatoma Hep G2 cell line*. *Toxicology*, 2000. **144**(1-3): p. 57-61.
61. Brigelius-Flohe, R., A. Banning, and K. Schnurr, *Selenium-dependent enzymes in endothelial cell function*. *Antioxidants & Redox Signaling*, 2003. **5**(2): p. 205-215.
62. Tappel, M.E., J. Chaudiere, and A.L. Tappel, *GLUTATHIONE-PEROXIDASE ACTIVITIES OF ANIMAL-TISSUES*. *Comparative Biochemistry and Physiology B-Biochemistry & Molecular Biology*, 1982. **73**(4): p. 945-949.

63. Schieber, M. and N.S. Chandel, *ROS Function in Redox Signaling and Oxidative Stress*. Current Biology, 2014. **24**(10): p. R453-R462.
64. Macfarlane, D.P., S. Forbes, and B.R. Walker, *Glucocorticoids and fatty acid metabolism in humans: fuelling fat redistribution in the metabolic syndrome*. Journal of Endocrinology, 2008. **197**(2): p. 189-204.
65. Letteron, P., et al., *Glucocorticoids inhibit mitochondrial matrix acyl-CoA dehydrogenases and fatty acid beta-oxidation*. American Journal of Physiology-Gastrointestinal and Liver Physiology, 1997. **272**(5): p. G1141-G1150.
66. Bassett, J.H.D., C.B. Harvey, and G.R. Williams, *Mechanisms of thyroid hormone receptor-specific nuclear and extra nuclear actions*. Molecular and Cellular Endocrinology, 2003. **213**(1): p. 1-11.
67. Liu, Q., A.S. Clanachan, and G.D. Lopaschuk, *Acute effects of triiodothyronine on glucose and fatty acid metabolism during reperfusion of ischemic rat hearts*. American Journal of Physiology-Endocrinology and Metabolism, 1998. **275**(3): p. E392-E399.
68. van der Vusse, G.J., *Albumin as Fatty Acid Transporter*. Drug Metabolism and Pharmacokinetics, 2009. **24**(4): p. 300-307.
69. Palace, V.P., et al., *Antioxidant potentials of vitamin A and carotenoids and their relevance to heart disease*. Free Radical Biology and Medicine, 1999. **26**(5-6): p. 746-761.
70. Sohal, R.S. and W.C. Orr, *The redox stress hypothesis of aging*. Free Radical Biology and Medicine, 2012. **52**(3): p. 539-555.
71. Traber, M.G. and J. Atkinson, *Vitamin E, antioxidant and nothing more*. Free Radical Biology and Medicine, 2007. **43**(1): p. 4-15.
72. Zhu, J., et al., *Physiological Oxygen Level Is Critical for Modeling Neuronal Metabolism In Vitro*. Journal of Neuroscience Research, 2012. **90**(2): p. 422-434.
73. Mach, W.J., et al., *Consequences of hyperoxia and the toxicity of oxygen in the lung*. Nurs Res Pract, 2011. **2011**: p. 260482.
74. Brand, M.D., *Mitochondrial generation of superoxide and hydrogen peroxide as the source of mitochondrial redox signaling*. Free Radical Biology and Medicine, 2016. **100**: p. 14-31.
75. Fu, T., et al., *Regulation of cell growth and apoptosis through lactate dehydrogenase C over-expression in Chinese hamster ovary cells*. Applied Microbiology and Biotechnology, 2016. **100**(11): p. 5007-5016.
76. Silva, L.P., et al., *Measurement of DNA Concentration as a Normalization Strategy for Metabolomic Data from Adherent Cell Lines*. Analytical Chemistry, 2013. **85**(20): p. 9536-9542.
77. NanoDrop. *NanoDrop Nucleic Acid Handbook*. 2010 [cited 2017 03 September].
78. Mulukutla, B.C., M. Gramer, and W.S. Hu, *On metabolic shift to lactate consumption in fed-batch culture of mammalian cells*. Metabolic Engineering, 2012. **14**(2): p. 138-149.
79. Le, H., et al., *Multivariate analysis of cell culture bioprocess data-Lactate consumption as process indicator*. Journal of Biotechnology, 2012. **162**(2-3): p. 210-223.
80. Halestrap, A.P. and M.C. Wilson, *The monocarboxylate transporter family - Role and regulation*. Iubmb Life, 2012. **64**(2): p. 109-119.
81. Liste-Calleja, L., et al., *Lactate and glucose concomitant consumption as a self-regulated pH detoxification mechanism in HEK293 cell cultures*. Applied Microbiology and Biotechnology, 2015. **99**(23): p. 9951-9960.
82. Francis, G.L., *Albumin and mammalian cell culture: implications for biotechnology applications*. Cytotechnology, 2010. **62**(1): p. 1-16.
83. Lu, S.C., *Regulation of glutathione synthesis*. Molecular Aspects of Medicine, 2009. **30**(1-2): p. 42-59.
84. Kohen, R., et al., *ANTIOXIDANT ACTIVITY OF CARNOSINE, HOMOCARNOSINE, AND ANSERINE PRESENT IN MUSCLE AND BRAIN*.

- Proceedings of the National Academy of Sciences of the United States of America, 1988. **85**(9): p. 3175-3179.
85. Drozak, J., et al., *Molecular Identification of Carnosine Synthase as ATP-grasp Domain-containing Protein 1 (ATPGD1)*. Journal of Biological Chemistry, 2010. **285**(13): p. 9346-9356.
 86. Lubos, E., J. Loscalzo, and D.E. Handy, *Glutathione Peroxidase-1 in Health and Disease: From Molecular Mechanisms to Therapeutic Opportunities*. Antioxidants & Redox Signaling, 2011. **15**(7): p. 1957-1997.
 87. Imlay, J.A., *Pathways of oxidative damage*. Annu Rev Microbiol, 2003. **57**: p. 395-418.
 88. Kador, P.F., J.H. Kinoshita, and N.E. Sharpless, *ALDOSE REDUCTASE INHIBITORS - A POTENTIAL NEW CLASS OF AGENTS FOR THE PHARMACOLOGICAL CONTROL OF CERTAIN DIABETIC COMPLICATIONS*. Journal of Medicinal Chemistry, 1985. **28**(7): p. 841-849.
 89. Brownlee, M., *Biochemistry and molecular cell biology of diabetic complications*. Nature, 2001. **414**(6865): p. 813-820.
 90. Trautwein, E.A. and K.C. Hayes, *TAURINE CONCENTRATIONS IN PLASMA AND WHOLE-BLOOD IN HUMANS - ESTIMATION OF ERROR FROM INTRAINDIVIDUAL AND INTERINDIVIDUAL VARIATION AND SAMPLING TECHNIQUE*. American Journal of Clinical Nutrition, 1990. **52**(4): p. 758-764.
 91. Kohlmeier, M., *Nutrient Metabolism: Structures , Functions and Genes*. 2015, Academic Press.
 92. Xu, W., et al., *Oncometabolite 2-Hydroxyglutarate Is a Competitive Inhibitor of alpha-Ketoglutarate-Dependent Dioxygenases*. Cancer Cell, 2011. **19**(1): p. 17-30.
 93. Jeong, D.W., et al., *Blocking of acidosis-mediated apoptosis by a reduction of lactate dehydrogenase activity through antisense mRNA expression*. Biochemical and Biophysical Research Communications, 2001. **289**(5): p. 1141-1149.
 94. Rae, C.D. and S. Broer, *Creatine as a booster for human brain function. How might it work?* Neurochemistry International, 2015. **89**: p. 249-259.
 95. Flanagan, J.L., et al., *Role of carnitine in disease*. Nutrition & Metabolism, 2010. **7**: p. 14.
 96. Jensen, J. and Y.-C. Lai, *Regulation of muscle glycogen synthase phosphorylation and kinetic properties by insulin, exercise, adrenaline and role in insulin resistance*. Archives of Physiology and Biochemistry, 2009. **115**(1).
 97. Bouskila, M., et al., *Allosteric Regulation of Glycogen Synthase Controls Glycogen Synthesis in Muscle*. Cell Metabolism, 2010. **12**(5): p. 456-466.
 98. Palm, D.C., J.M. Rohwer, and J.H.S. Hofmeyr, *Regulation of glycogen synthase from mammalian skeletal muscle - a unifying view of allosteric and covalent regulation*. Febs Journal, 2013. **280**(1): p. 2-27.
 99. Shafiei, M.T., et al., *Detecting Glycogen in Peripheral Blood Mononuclear Cells with Periodic Acid Schiff Staining*. Jove-Journal of Visualized Experiments, 2014(94): p. 8.